Human decision-making at roundabouts: The role of gaze movements, velocity and distance to gap in gap acceptance

by

Mohamed Elsayed

to obtain the degree of Master of Science
at the Delft University of Technology,
to be defended publicly on Thursday April 17, 2025 at 09:00 AM.

Student number:	4725255	
Project duration:	July 21, 2024 – April 17, 2025	
Thesis committee:	Dr. Arkady Zgonnikov	TU Delft, supervisor
	Ir. Federico Scarí	TU Delft, supervisor
	Dr. Yan Feng	TU Delft, external member

Human decision-making at roundabouts: The role of gaze movements, velocity and distance to gap in gap acceptance

Mohamed Elsayed

Department of Cognitive Robotics, Delft University of Technology, Faculty of ME

Abstract—Understanding how human drivers interact in dynamic traffic situations is a crucial step toward the safe and seamless integration of automated vehicles (AVs) into everyday traffic. A common setting for these interactions is the four way single-lane roundabout. Here, drivers must make quick decisions about who yields and who proceeds, based not just on traffic rules but also on subtle cues and shared expectations. These decisions rely heavily on gap acceptance, where each driver evaluates whether there is enough space and time to enter the roundabout safely. It often depends on mutual negotiation and split-second judgments, shaped by visual contact and behavioral feedback. While earlier studies have explored driver gaze behavior in controlled environments, little is known about how gaze correlates with decision-making in continuous and mutual encounters, especially at roundabouts. This study fills that gap by studying human-human interactions during roundabout entry in a novel experimental setup. Using a coupled virtual reality driving simulator, two participants navigated a single-lane roundabout under varying approach speeds and distances. Eye-tracking was used to measure where and how long each driver fixated at the other vehicle. Control input data captured how drivers reacted in the seconds following these gaze events. The results show that both entry distance and speed had a strong influence on who proceeded first. Drivers who started closer to the roundabout or moved faster were more likely to take priority. Drivers positioned closer to the conflict zone looked at the other vehicle for longer durations, indicating stronger visual engagement. Furthermore, drivers often responded with throttle or brake inputs shortly after looking at the other vehicle, especially when distance to the roundabout was small. This study offers insight into how gaze behavior, positioning and control decisions shape mutual negotiation at roundabouts. These findings move beyond the idea of gap acceptance as a one-sided decision and highlight the importance of real-time interaction.

Index Terms— Roundabout, Human-Human interaction, Decision-making, Driving simulator, Coupled simulator

1 INTRODUCTION

The rise of automation and intelligent systems has started to transform the way transportation systems are designed and used. In recent years, technological advances in automated vehicles (AVs) have opened new possibilities for reshaping how we move, with the potential to make transportation safer, more efficient and accessible to a broader range of users [1–4]. Governments and industry leaders increasingly view AVs as a key solution to long-standing and future transportation challenges [5]. Although early advances suggest that AVs could improve road safety by reducing human error, it is not yet clear to what extent they can eliminate traffic risks [6]. Human error is frequently cited as the primary factor in up to 94 percent of traffic accidents [7]. But this statistic oversimplifies the complexity of driver behavior [7, 8]. Many accidents attributed to human error do not result solely from impaired driving. They also stem from factors such as driver inattention, limited situational awareness or errors in judgment that automated vehicles may also fail to resolve [9]. To successfully integrate AVs into existing traffic systems, it is essential to gain a deeper understanding of human driving behavior. Since AVs must operate alongside human drivers, this requires the ability to interpret and anticipate human decisions in dynamic situations such as unprotected left turns, lane merges and entries into roundabouts [10]. This understanding also plays a key role in addressing ongoing concerns about AV safety [11, 12].

While AV technology continues to evolve, roundabouts have long played a central role in road design and have seen wider implementation in recent years as a proven method to improve traffic flow and safety [13, 14]. This effectiveness results from their ability to reduce vehicle delays and force drivers to lower their speed when approaching the intersection. These effects lead to measurable safety improvements. Compared to traditional intersections, roundabouts reduce injury-related crashes by 72 to 80 percent and lower total crash numbers by 35 to 47 percent [15, 16]. As both AV technology and roundabout use grow, their successful integration into existing infrastructure remains necessary to fully realize their benefits and to build public confidence in their implementation [17, 18].

In roundabout maneuvering, gap acceptance is a critical decision-making process where drivers must judge whether traffic gaps are sufficient for safe entry. Traditional studies often treat gap acceptance decisions as instantaneous, which overlooks their complex and time-dependent nature [19, 20]. In practice, drivers base their judgments on a combination of factors such as relative speed, approach distance and the actions of other road users [21]. Importantly, gap acceptance is not the result of an isolated judgment by a single driver but results from the interaction between at least two road users, each influencing the other's decision through their actions and responses. These interactions depend on continuous mutual awareness. This dynamic process reflects the broader nature of traffic interactions, which evolve constantly in response to cues [22]. These cues can include both explicit forms of communication such as indicators, vehicle speed and trajectory and implicit ones such as gaze direction, head movements and subtle vehicle positioning [23, 24].

Despite the central role of communication in driver interactions, existing research often treats decision-making as a one-sided process and gives limited attention to the communicative cues that guide mutual behavior. This narrow focus restricts our understanding of the complexity involved in real-world human-human interactions, particularly in scenarios like roundabouts [25]. While direct communication between drivers at a roundabout is limited, much of the interaction depends on how drivers interpret the movements and positioning of surrounding vehicles. In this context, gaze behavior offers valuable insight into how drivers gather information, track other vehicles and make split-second decisions based on their perception of the traffic environment [26].

Previous studies has examined how factors such as speed and environment influence gaze allocation and driver attention [27, 28], as well as the duration and timing of fixations during specific driving tasks [29, 30]. Additional work has explored traffic flow, safety and driving comfort of automated vehicles at roundabouts [31], but no studies have investigated how gaze behavior and mutual driver interaction occur within this specific context. Research that considers how drivers influence one another in shared traffic situations remains limited, partly because these interactions are difficult to study and safely reproduce in real-world conditions. A study by Scarí et al. [32] tried to overcome this limitation by using a coupled driving simulator to examine mutual driver behavior and driver workload, but this work focused solely on highway merging. Although existing studies provide valuable insights into driver gaze behavior [33], little attention has been given to its role in roundabout scenarios that involve multiple interacting drivers. Addressing this gap is essential for developing more accurate and realistic models that better reflect real-world traffic dynamics. These improvements can ultimately support the integration and acceptance of AVs in mixed traffic environments such as roundabouts [10, 12].

To address the gap identified in the research, this study investigates the following main research question:

How does driver gaze behavior correlate with mutual decision-making and driver control during gap acceptance at roundabouts?

To explore this question comprehensively, this study analyzes how human drivers make gap acceptance decisions at roundabouts by examining the role of gaze behavior in mutual interactions. It considers the influence of head and eye movements, the effects of varying approach speeds and distances to the yield line and how driver control inputs change following gaze fixations on other vehicles. Furthermore, the study investigates the following sub-questions:

1) How do variations in entry speed and approach distance influence driver gap acceptance behavior?
2) How does the frequency and duration of fixations on other vehicles vary with entry speed and approach distance?
3) What is the relationship between gaze data and a driver's decision to accept or reject a gap at a roundabout?
4) How does driver control change after a fixation on another vehicle?

To answer these research questions, we conducted a controlled human-human interaction experiment in a coupled Virtual Reality (VR) environment. This setup allowed two participants to interact with each other in simulated driving scenarios, which provides detailed insights into how drivers assess gaps, interact with each other and decide whether to yield or proceed at roundabouts.

2 METHOD

2.1 Sample characteristics

Approval for this study was granted by the Human Research Ethics Committee of Delft University of Technology. A total of ten healthy adult participants (Mean = 23.6 years, SD = 3.0 years) took part in the study, divided into pairs over five sessions. Each session involved a randomly assigned pair of participants. The pairs did not know each other before the experiment, which minimized potential biases due to familiarity. The group consisted of six males and four females. All participants held a valid Dutch driver's license, with an average driving experience of 4.5 years (SD = 2.5 years). Prospective participants were screened for eligibility based on their susceptibility to motion sickness. Participants reporting susceptibility to motion sickness did not participate in the study. After meeting the criteria, participants received a detailed consent form and provided informed consent before participation. Most participants were students or researchers affiliated with TU Delft.

2.2 Experimental design

To gather experimental data, a controlled human-human experiment was conducted using a VR environment, see Figure 1 for a detailed top-down overview and explanation of the map. Participants were explicitly instructed to drive according to their typical driving behavior during roundabout maneuvers and informed that their interaction would occur solely with their assigned partner. Participants could not see each other until reaching a specific point near the roundabout. Participants were also prohibited from communicating verbally during the trials. To enforce this restriction, participants wore noise-cancelling headphones throughout the experiment.

Before starting the actual experiment, participants performed several practice trials to familiarize themselves with the vehicle dynamics, the experimental setup and the virtual environment. These practice trials featured slightly varied and randomized conditions compared to the actual experiment to account for potential learning effects and to minimize the influence of uncontrolled variables.

The experiment featured a first-person perspective within a virtual vehicle, see Figure 2. This was done to provide participants with the immersive feeling of being

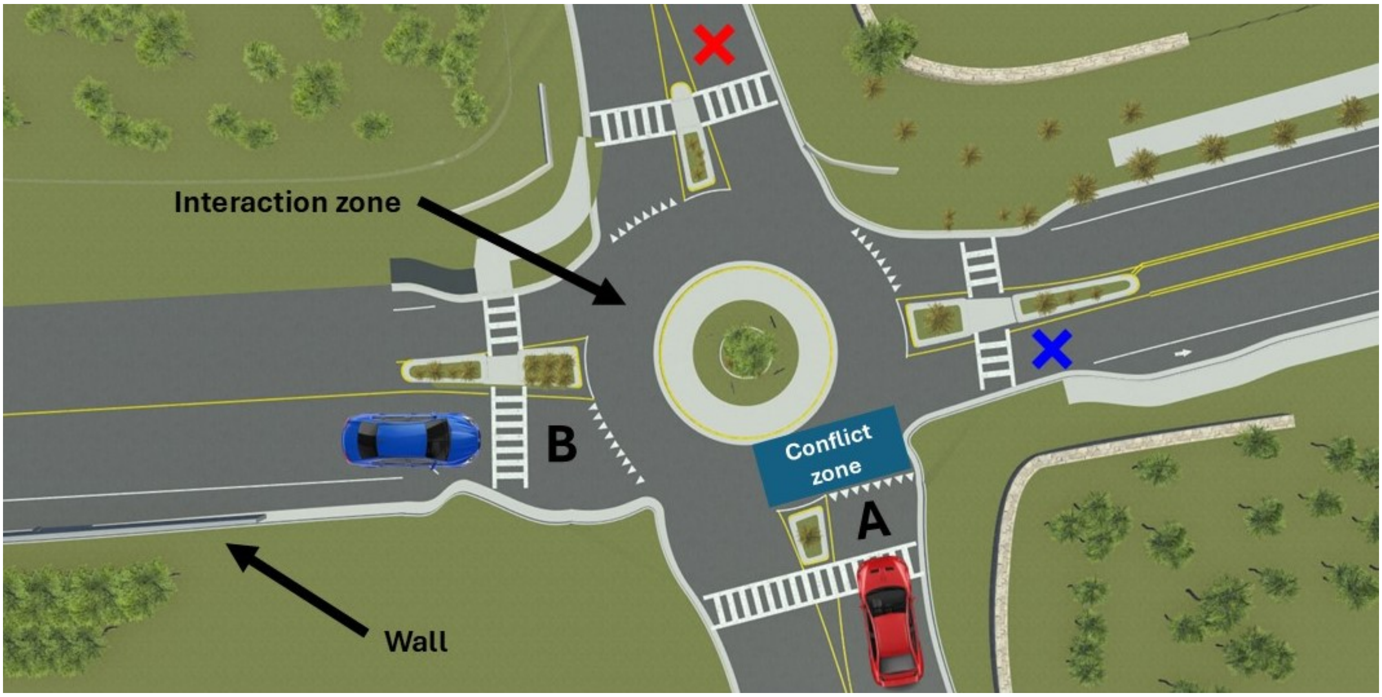

Figure 1: Top-down view of the single-lane, four-way roundabout map. The Figure illustrates the red vehicle approaching from Road $\mathcal{A}$ (the south road) and the blue vehicle from Road $\mathcal{B}$ (the west road). A wall positioned next to Road $\mathcal{B}$ restricts the visibility of both drivers towards each other. This wall simulates a realistic scenario where drivers can see each other only when approaching the roundabout. The interaction zone is defined as the area within the roundabout, behind the yield lines. The conflict zone is the specific area immediately after the yield line of Road $\mathcal{A}$. The dimensions of the conflict zone are 10 m in width and 5 m in length. This location determines which vehicle enters first, concluding the interaction between drivers.

inside an actual vehicle. The virtual environment was designed as a single-lane, four-way roundabout. Each trial began from one of two predetermined entry roads. The two entry roads were from the south and west. In Figure 1 the roads are illustrated as Road $\mathcal{A}$ and Road $\mathcal{B}$. The trials were randomized as part of the experimental design. Participants received instructions to always take the second exit, as illustrated in Figure 1, where the second exit is marked with an X corresponding to the color of each car. This procedure aimed to reduce motion sickness potentially caused by excessive turns.

Figure 2: A first-person perspective from within the virtual vehicle used during the experiment. In this Figure, the driver, coming from Road $\mathcal{A}$, whose point of view is depicted is yielding at the roundabout to the other driver who is circulating within it.

Initially, participants controlled only the steering of their vehicle on the straight roadway segment leading up to the roundabout, with the vehicles operating under cruise control. At a specific moment (see Section 2.4) before reaching the roundabout, both participants received simultaneous an auditory cue. This cue signals the transition to full manual control. This includes throttle, brake and steering. Participants then approached and navigated the roundabout using full manual control. Participants were able to see their velocity in front of them on the car dashboard. Each trial ended when one participant reached a predetermined distance beyond the roundabout. After each trial, participants re-initialized at the designated starting location for the next trial.

Each trial involved three controlled variables: the approach distance, the approach velocity to the yield line at the roundabout as well as the designated road. These variables resulted in a fully factorial 2 x 2 x 2 design, creating 8 unique experimental conditions. Trials were evenly distributed across four sessions, each consisting of 20 trials. Each session lasted approximately 10 minutes and included a 5-minute break between sessions to allow participants time to recover and reduce fatigue and potential motion sickness.

2.3 Setup

The experiment was conducted in a driving simulator at the Cognitive Robotics Department of Delft University of Technology. Participants controlled the virtual vehicle using a Logitech G923 TRUEFORCE sim racing wheel and pedals. To provide an immersive, high-resolution visual environment and advanced eye-tracking capabilities, a Varjo VR3 VR headset was employed. The virtual driving environment was created using Unreal Engine 4.26 in combination with

CARLA 0.9.13, an open-source autonomous driving simulation platform [34]. The environment map was designed using Mathworks RoadRunner 2024 [35] and subsequently imported into CARLA. Data recording and experiment management were handled through JOAN [36], an open-source software framework that captures experimental data at a sampling rate of 100 Hz. Figure 4 illustrates the complete experimental setup.

2.4 Experimental conditions

Two drivers simultaneously approached the roundabout from two different directions. Driver 1 approached from Road $\mathcal{A}$ and driver 2 approached from Road $\mathcal{B}$, see Figure 1 as an example of the first condition. Both drivers started from a stationary position, accelerated and continued under cruise control until one of the participants reached a predefined distance of 50 meters from their initial starting point. The driver who reached this reference point first was always the one traveling at a higher initial velocity. The other driver reached a distance of 40 meters. At this moment, both drivers simultaneously gained full control of their vehicles. Steering inputs, braking and acceleration were then permitted. During the experiment, participants were instructed to drive around 25 km/h when navigating the roundabout, to combat motion sickness when turning.

The initial conditions for each trial included two controlled variables: the drivers' starting positions (distance to the yield line) and the vehicle speed upon reaching the reference point. Drivers began either at 85 meters or 72 meters from their respective yield lines, creating a spatial offset of either +6 meters (back) or -6 meters (front) from the reference point at 78.5 meters. Additionally, vehicle speeds were adjusted relative to a baseline of 40 km/h, resulting in one driver traveling at 44 km/h (+4 km/h, fast) and the other at 36 km/h (-4 km/h, slow). These initial conditions were defined through trial and error to ensure that approximately half of the scenarios led to a challenging interaction, where it was not clear who would go first. The other half formed less ambiguous situations that acted as control conditions. This approach produced a mix of cases: in some, it was clear which driver had priority; in others, the outcome depended on the actions and interactions of the drivers.

This resulted in the two experimental manipulations to be defined as:

1) **Spatial Offset ($\frac{1}{2}\Delta d$)**: adjusted by either -6 meters (front) or $+6$ meters (back), resulting in either a decreased or increased gap.
2) **Velocity Offset ($\frac{1}{2}\Delta v$)**: adjusted by either -4 km/h (slow) or $+4$ km/h (fast), resulting in velocities of 36 km/h or 44 km/h.

The drivers always experienced opposite conditions. When one driver started closer to the yield line (front), the other started further away (back). Similarly, when one driver approached at a higher velocity (fast), the other approached at a lower velocity (slow). Table 1 summarizes these experimental conditions.

Table 1: Conditions from the perspective of both drivers. The conditions for both drivers are always flipped. 4 conditions × 2 configurations due to road switching

Condition	Driver Road $\mathcal{A}$	Driver Road $\mathcal{B}$
c1	$-6\,\text{m},\ -4\,\text{km/h}$	$+6\,\text{m},\ +4\,\text{km/h}$
c2	$-6\,\text{m},\ +4\,\text{km/h}$	$+6\,\text{m},\ -4\,\text{km/h}$
c3	$+6\,\text{m},\ -4\,\text{km/h}$	$-6\,\text{m},\ +4\,\text{km/h}$
c4	$+6\,\text{m},\ +4\,\text{km/h}$	$-6\,\text{m},\ -4\,\text{km/h}$

Figure 3 illustrates a top-down view of the different configurations during the experiment and the end goal of the drivers.

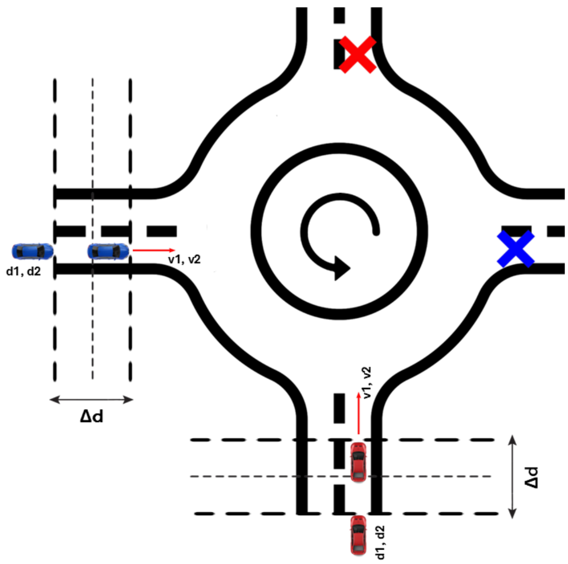

Figure 3: Top-down view of the experimental conditions. Each driver experienced opposite conditions. Drivers started at either position d1 or d2 and approached with velocities v1 or v2, representing two distance and two velocity settings

In total, the experimental design consisted of 8 unique experimental conditions (4 conditions × 2 configurations due to road switching). Each condition was repeated 10 times in randomized order, resulting in 80 trials per participant and a total of recorded 800 trials across all five experiments (80 trials × 5 experiments × 2 participants per trial). The Latin Square method was employed throughout the experiment to ensure balanced representation and controlled experimental conditions. For clarity and readability, in the remainder of this paper, we refer to -6 m as *front*, +6 m as *back*, -4 km/h as *slow* and +4 km/h as *fast*.

2.5 Exclusion criteria

Trials that involved collisions (n = 8, representing 1% of the total data) were excluded from the analysis. This decision was made because the research specifically focused on successful driver interactions at roundabouts. Collisions represented fundamental breakdowns in interaction and provided limited insights into typical driver behavior.

Additionally, data analysis was limited to the period between the moment participants gained vehicle control and the entry of one driver into the conflict zone. After this point, the interaction outcome became clear and thus offered no further insight into mutual driver reactions or gaze patterns.

Figure 4: Experimental setup depicting two participants seated facing opposite directions, separated by curtains to prevent visual contact. Each participant had access to a steering wheel and gas and brake pedals positioned directly in front of them. Participants wore Varjo Base headsets and noise-cancelling headphones throughout the experiment. Both participants' views were continuously monitored through separate displays to ensure proper system functioning and participant compliance.

2.6 Data collection

2.6.1 Vehicle data

Vehicle data were recorded using JOAN at a sampling frequency of 100 Hz. The collected data included timestamps and driver inputs such as steering angle, throttle and brake. Additionally, vehicle-specific data was recorded. This includes velocity and acceleration in both vehicle and world reference frames, along with positional coordinates (X, Y, Z) and rotational angles (Yaw, Pitch, Roll) for each vehicle.

2.6.2 Gaze data

Eye-tracking data were recorded using the Varjo Base headset at a sampling frequency of 100 Hz. The collected data included timestamps, head rotation angles and gaze positions. The head rotation angles were provided in degrees, where positive values corresponded to rightward head movements. Gaze data were recorded initially as positional coordinates (X, Y, Z) and subsequently transformed into gaze angles to represent the driver's left and right visual orientation.

2.6.3 Data synchronization

Vehicle data from JOAN and the gaze data from the Varjo Base headset were collected at a frequency of 100 Hz. JOAN recorded each trial separately, with timestamps initiated at the start of each trial. In contrast, the Varjo Base headset recorded continuous data for each session of 20 trials, with a timestamp initiated at the start of the initialization script. A post-processing script matched and synchronized JOAN trial data to the corresponding Varjo data based on timestamps. Rows without corresponding data from both JOAN and Varjo were removed. After synchronization, data from all four sessions were combined into a single dataset per participant. This synchronization process was repeated separately for each participant, resulting in two synchronized datasets per participant pair.

2.7 Gaze data validation

This study aimed to determine when a driver's fixation was directed precisely toward the other vehicle. This information reveals the frequency and duration of fixations while drivers approached and navigated the roundabout. To accurately measure this behavior, two criteria were defined:

1) **Visibility Criterion:** To prevent drivers from viewing each other prematurely, a static wall was positioned next to the road, as illustrated in Figure 1. Due to the static nature of this barrier, the moment the drivers could see each other could analytically be determined through two calculations. First, the relative angle between the two vehicles was computed. Then, the relative angle from the vehicle on Road $\mathcal{A}$ to the outer edge of the wall was calculated. Drivers could see each other once the vehicle-to-wall angle was equal to or greater than the vehicle-to-vehicle relative angle. An assumption made here is that both drivers can see each other at the same time. In reality, a small time difference may exist, but this was considered negligible.

2) **Gaze Angle Criterion:** To analyze driver gaze behavior, both the central gaze, which includes head rotation and eye movement and the peripheral vision that contributes to situational awareness were considered. Drivers rely on foveal vision for sharp focus and peripheral vision to detect environmental changes [37]. However, identifying whether a driver's gaze was precisely focused on the other vehicle required accounting for the size of the object within the driver's foveal vision, which varied based on distance. Specifically, objects farther away occupied smaller gaze angles, while closer objects occupied larger gaze angles.

To determine if a driver's gaze was precisely focused on the other vehicle, the effective gaze angle was calculated as:

$$G_{\text{effective}} = H + E + 2\theta \tag{1}$$

where:

- H = Head rotation angle (degrees)
- E = Eye rotation angle (degrees)
- θ = Angular range (degrees, per side)

To calculate the angular range within which the other vehicle falls into a driver's effective gaze, the following formula was used:

$$\theta = 2 \times \arctan\left(\frac{s}{2 \times d}\right) \tag{2}$$

where:

- θ = Angular range of the driver's effective gaze (degrees)
- s = Width of the car (meters)
- d = Euclidean distance between the two vehicles (meters)

This calculation was performed continuously from the moment drivers first became visible to each other until one vehicle entered the conflict zone. The angular range is thus dynamically scaled with distance. This enables a precise determination of when a driver was precisely fixating on the other vehicle. This calculated angular range constituted the driver's effective gaze. Figure 5 illustrates the definitions of head rotation angle, eye rotation angle and the angular range corresponding to the effective gaze.

2.8 Metrics

Four primary metrics were defined to quantify driver interactions during the experiment:

1) The order in which the drivers entered the conflict zone (see Figure 1) was used to determine which driver went first and which one yielded.
2) The number of fixations each driver made toward the other vehicle.
3) The total fixation duration each driver directed toward the other vehicle throughout each trial.
4) The control input by each driver. This includes using the throttle, brake or not giving any input.

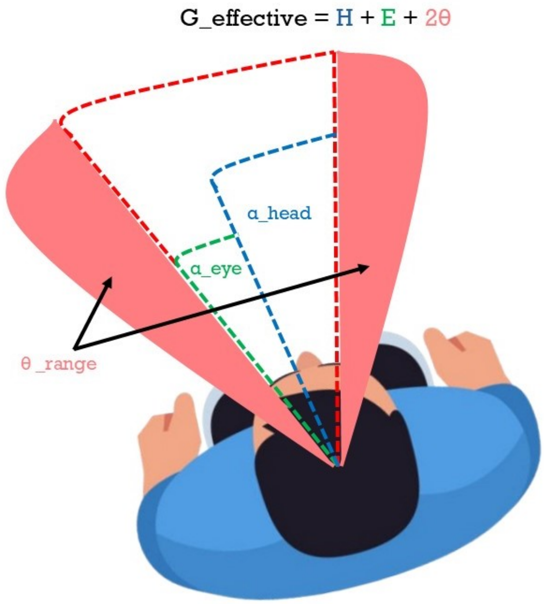

Figure 5: The figure illustrates the components that constitute the effective gaze angle. The eye angle is marked in green and the head angle in dark blue. The combined head and eye angle is represented in red. The angular range is displayed on both sides in coral. Together, these three components form the effective gaze angle of a driver. The illustration is adapted from Scarí et al. [32] and adjusted accordingly.

2.9 Fixation count and duration extraction

For every trial, we collected the fixation counts and total fixation time. Figure 6 shows an example of the processed data. The explanation refers only to the upper part of the figure, since the same logic applies to the lower part as well. The relative angle between the vehicles on Road $\mathcal{A}$ and Road $\mathcal{B}$ is shown as a blue line. The raw head and eye gaze data were combined and smoothed to produce a continuous combined gaze angle. The range around the combined gaze angle, representing the functional field of view, varied in size. This variation followed the method described in Section 2.7 under the second criterion. The black dashed line marks the moment when both drivers received manual control of their vehicles. This occurred when one of the drivers, always the one with the higher velocity, reached a distance of 50 meters. The orange line indicates when both drivers could see each other. This moment depended on the experimental conditions and followed the visibility criterion in Section 2.7. The grey dashed line shows when one of the participants entered the conflict zone.
All event markers were added to the plot. Between the orange and grey lines, the functional field of view is scaled dynamically based on the distance between the vehicles. In Figure 6, the range is small at the beginning and increases rapidly. Fixation intervals were determined by identifying times when the relative angle between the vehicles fell within the scaled range. A dot marks the start of each fixation and a cross marks the end. The script counted the number of fixations and calculated their total duration. Both values are shown in the figure. The durations of individual fixations were also saved but are not shown in the plot.

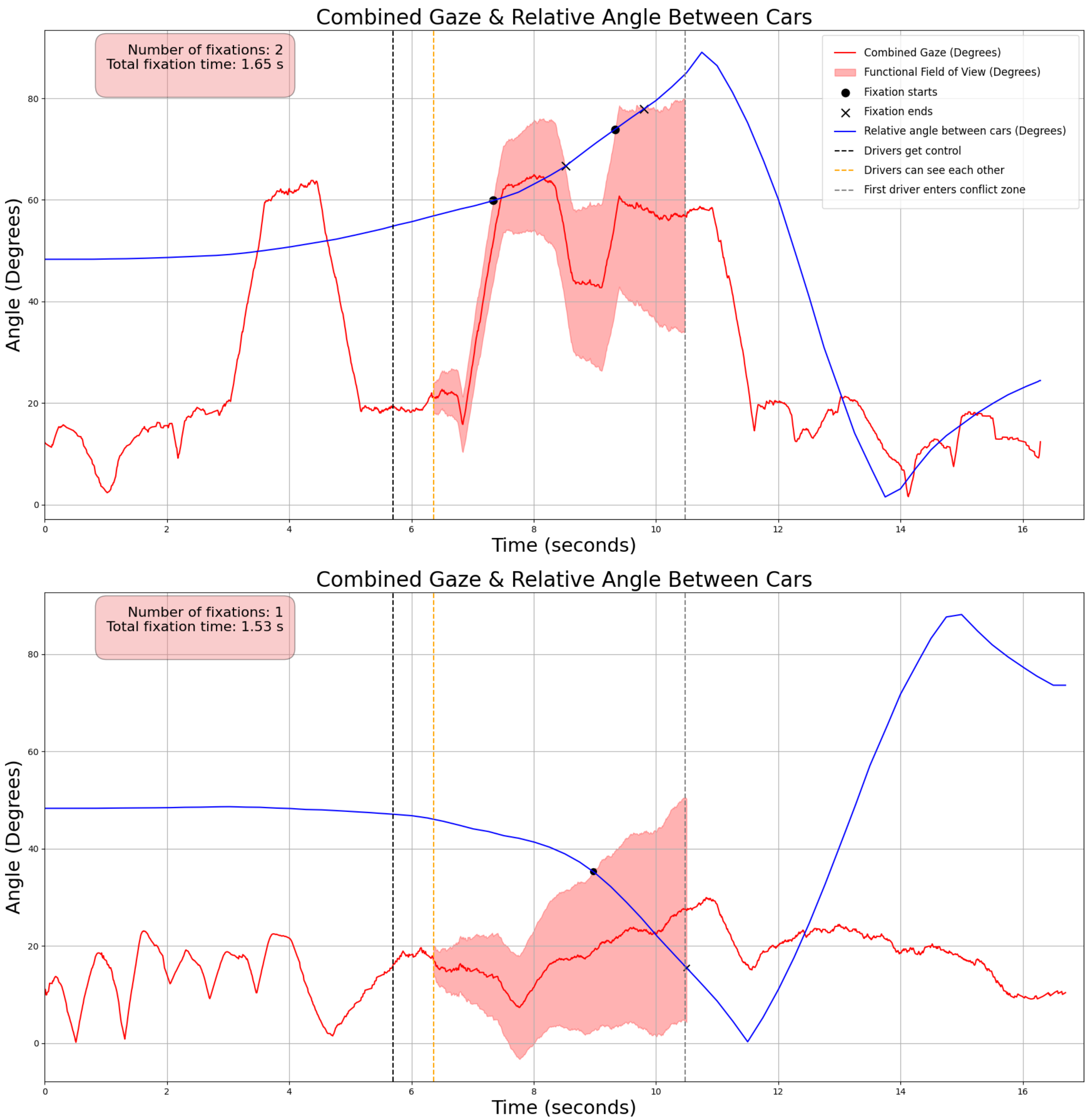

Figure 6: Combined gaze angle and relative angle between the vehicles over time. The red line shows the combined gaze angle, while the shaded red area indicates the functional field of view (effective gaze). The driver in the upper part of the figure, approaching from Road $\mathcal{B}$, is looking to the right, which corresponds to a positive gaze angle. The driver in the lower part of the figure, approaching from Road $\mathcal{A}$, is looking to the left. To facilitate comparison, negative combined gaze values were converted to absolute values. The blue line represents the relative angle between the vehicles from roads A and B, which was also converted to an absolute value. Vertical dashed lines indicate key events: the moment drivers gained control of the vehicles (black), the point at which they became visible to each other (orange) and the moment the first driver entered the conflict zone (grey). Fixation intervals were defined based on the overlap between the relative angle and the functional field of view. In this figure, two fixations were identified for the driver on Road $\mathcal{B}$, marked by black circles (start) and black crosses (end). One fixation was identified for the driver approaching from Road $\mathcal{A}$. The data shown correspond to trial 121 which corresponds to the third condition, see Table 1

2.10 Control input extraction

The control input data used in this study , which includes only braking and accelerating, follows from the fixation data extracted as described in Section 2.9. The recorded fixation time served as the basis for identifying the relevant control input from each driver. The first point of extraction corresponded to the start of the fixation. The second point represented the driver's reaction time to the observed stimulus. This study assumes a reaction time of 0.75 seconds, based on values reported in [38, 39], which identified reaction times

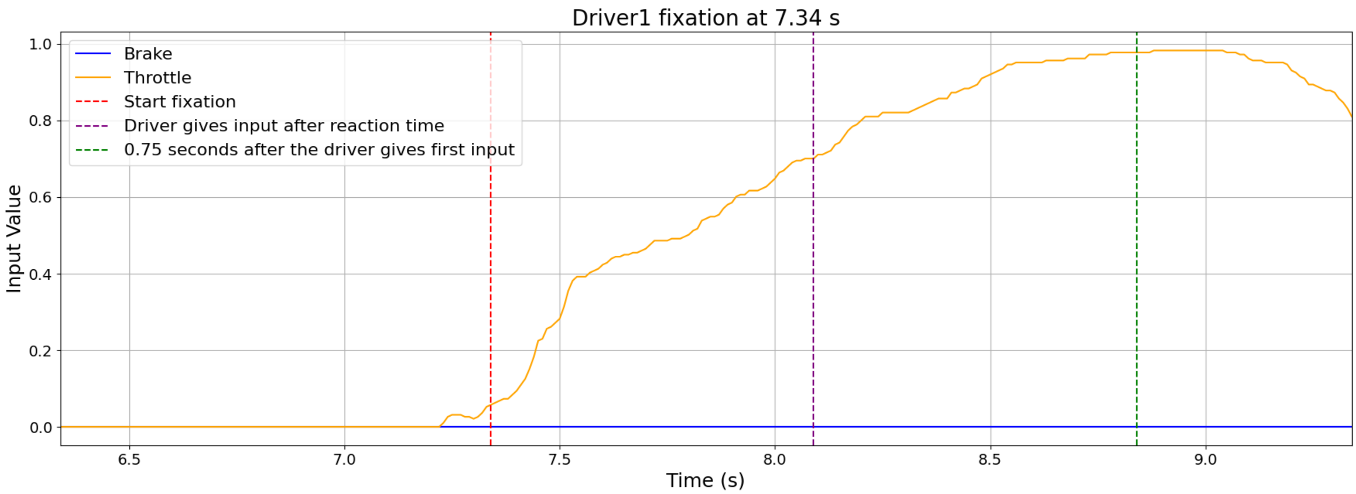

Figure 7: This figure shows driver 1's pedal inputs (brake in blue, throttle in orange) from one second before the start of the fixation at 7.34s until two seconds afterward. The red dashed line marks the start of the fixation, the purple dashed line indicates 0.75s later when the driver first applies a control input as a result of the fixation and the green dashed line indicates an additional 0.75s later. The throttle rises from 0.06 at the start of the fixation to 0.70 at 8.09s and then to 0.98 at 8.84s, while the brake remains at 0.0 throughout this interval. This control input corresponds to the first fixation shown in Figure 6 for driver 1.

of 0.732 and 0.77 seconds respectively for attentive drivers. The average of these values was adopted for consistency. The final point was recorded 0.75 seconds after the first control input. These three key time points were extracted to compare the driver's control actions before and after fixation. An example of the extracted control input is shown in Figure 7.

2.11 Statistical analysis

We conducted statistical analyses using mixed-effects regression models to account for the repeated measures structure of the data. To model the binary outcome of *which driver entered the conflict zone first*, we employed logistic regression with a Bernoulli family using Bambi [40]. The fixed effects included spatial offset (Δd), speed offset (Δv) and road. The road variable was included to account for potential asymmetries in driver behavior between Road $\mathcal{A}$ and Road $\mathcal{B}$. We also incorporated random intercepts and slopes per participant, which allowed the model to capture individual variability in baseline decisions and sensitivity to spatial and velocity changes. Including these random effects improved the model fit by accounting for dependencies among repeated observations per participant. The z-values and associated p-values were derived from posterior distributions.

To analyze *the number of fixations* drivers made toward the other vehicle, we applied a linear mixed-effects model with `statsmodels` [41]. Spatial offset (Δd), speed offset (Δv), road and whether the driver went first were treated as fixed effects. A random intercept for each participant was included to control for individual differences in gaze behavior across trials. We used a similar linear mixed-effects approach to model the *total fixation duration* and employed an identical structure of fixed and random effects.

For the control inputs, histograms were generated and transformed into probability densities to display the distribution of the inputs made by the driver following the fixations. This was done separately for different but equal distances from the conflict zone. These histograms provided a visual representation of the drivers' control actions, allowing us to compare how control inputs vary relative to spatial proximity to the conflict zone.

We summarized the results by calculating coefficient estimates, standard errors, z-values and p-values. The significance level was set at $p < 0.05$.

3 RESULTS

This chapter shows the results of driver behavior at the roundabout. It includes which driver passed first through the conflict zone, the number of fixations, total fixation time and control inputs by the drivers. The outcomes for driver priority are shown separately for Road $\mathcal{A}$ and Road $\mathcal{B}$. The number of fixations and their duration were extracted as shown in Section 2.7. Control inputs were used to assess how drivers changed their behavior after fixating towards the other vehicle. Eight trials were excluded due to collisions. These represented about 1% of the data.

3.1 Driver priority at the conflict zone

A total of 392 trials were included in the analysis. The probability that a driver proceeded first through the conflict zone was influenced by both spatial and velocity offsets. Figure 8 illustrates how changes in initial distance ($\frac{1}{2}\Delta d$) and speed ($\frac{1}{2}\Delta v$) affected yielding behavior. Drivers with an initial speed advantage were more likely to proceed first, particularly when also positioned closer to the conflict zone. This pattern held for drivers on both Road $\mathcal{A}$ and Road $\mathcal{B}$. For example, when the driver on Road $\mathcal{A}$ had both spatial and velocity advantage, the probability of going first reached 0.90. However, when both factors were unfavorable, the probability dropped to 0.08.

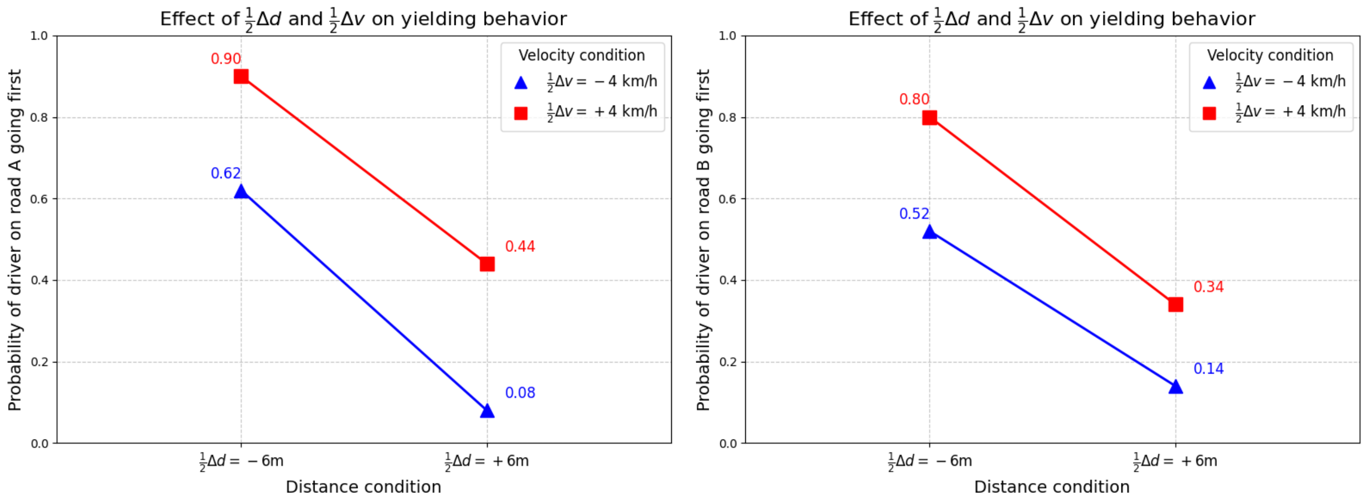

Figure 8: Effect of $\frac{1}{2}\Delta d$ and $\frac{1}{2}\Delta v$ on yielding behavior. The left plot shows the probability of the driver on Road $\mathcal{A}$ going first. The right plot shows the probability of the driver on Road $\mathcal{B}$ going first. Red squares indicate the condition with increased velocity ($\frac{1}{2}\Delta v = +4$ km/h) and blue triangles indicate the condition with decreased velocity ($\frac{1}{2}\Delta v = -4$ km/h).

These patterns are statistically supported by the logistic mixed-effects model shown in Table 2. Spatial offset had a strong negative effect on the likelihood of proceeding first ($z = -8.143$, $p < 0.001$), with a 95% confidence interval of $[-0.141, -0.087]$. Velocity offset had a significant positive effect ($z = 3.846$, $p < 0.001$), with a 95% confidence interval of $[0.049, 0.151]$. These findings confirm that both proximity and speed advantage significantly increase the probability of a driver taking priority at the roundabout.

Table 2: Results of the Logistic Mixed-Effects Model Predicting Driver Priority at the Conflict Zone. The Model Included Spatial Offset, Velocity Offset and Road $\mathcal{A}$s Fixed Effects, with Random Slopes per Participant for Spatial and Velocity Offsets.

Variable	Estimate	Std. Error	z-value	p-value
Intercept	0.148	0.123	1.203	0.229
Δd	-0.114	0.014	-8.143	< 0.001
Δv	0.100	0.026	3.846	< 0.001
Road $\mathcal{B}$	-0.297	0.154	-1.929	0.0538

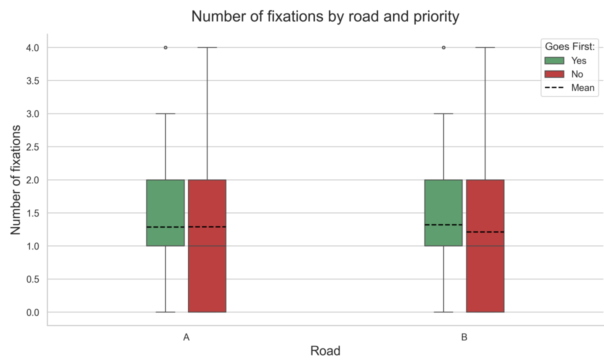

Figure 9: Number of fixations per road, separated by whether the driver went first through the conflict zone. Green bars represent trials in which the driver went first and red bars represent trials in which the driver yielded. The dashed black lines indicate the mean number of fixations.

Figure 10: Total fixation time per road, separated by whether the driver went first through the conflict zone. Green bars represent trials in which the driver went first and red bars represent trials in which the driver yielded. Individual data points for each trial are shown and the dashed black lines indicate the mean fixation time.

3.2 Fixation count and duration

Across both roads, drivers who went first and those who yielded showed similar numbers of fixations. Figure 9 presents the total number of fixations per trial, separated by whether the driver proceeded first and by road. Median values and interquartile ranges are comparable across all conditions. While outliers are present, they are distributed relatively evenly. The data includes all recorded trials from all participants.

In contrast, total fixation time showed more visible variation across conditions. Drivers who yielded tended to spend slightly more time fixating on the other vehicle, although variation remained high across both roads. These differences are illustrated in Figure 10, where individual data points highlight the spread within each group. The distributions reflect all participants and trials, grouped by road and driver priority.

Fixation behavior did not significantly predict which driver proceeded first. In the model predicting the number of fixations, the variable indicating who went first was not a significant predictor ($p = 0.685$). Similarly, in the model

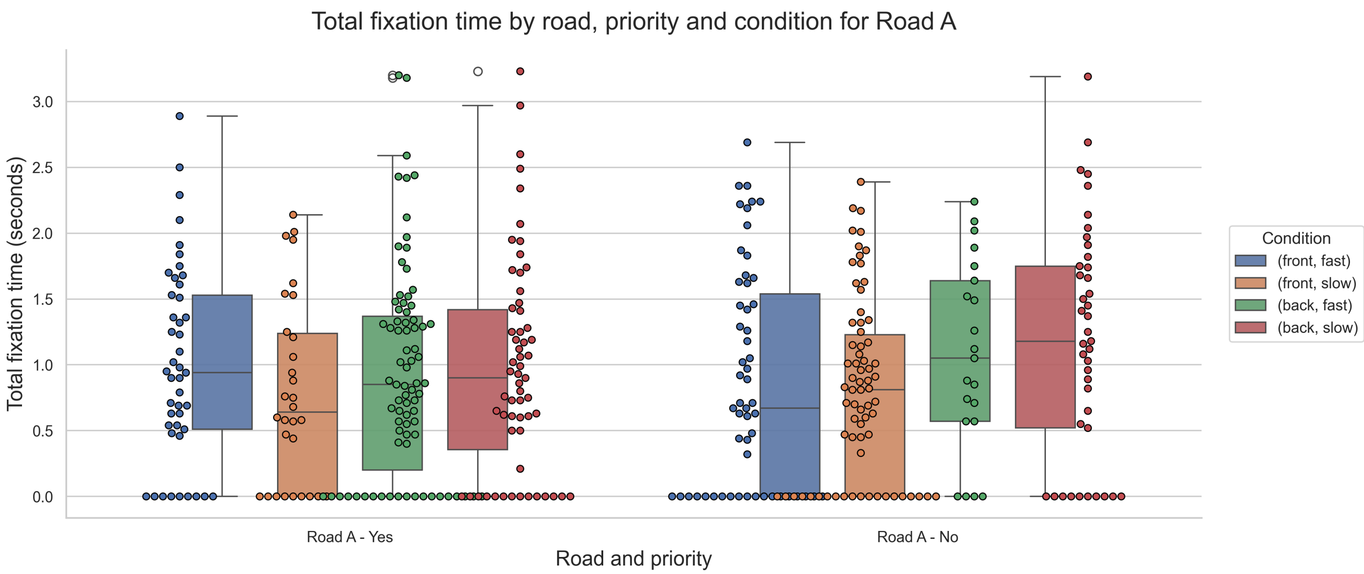

Figure 11: Total fixation time for Road $\mathcal{A}$, grouped by condition and whether the driver went first.

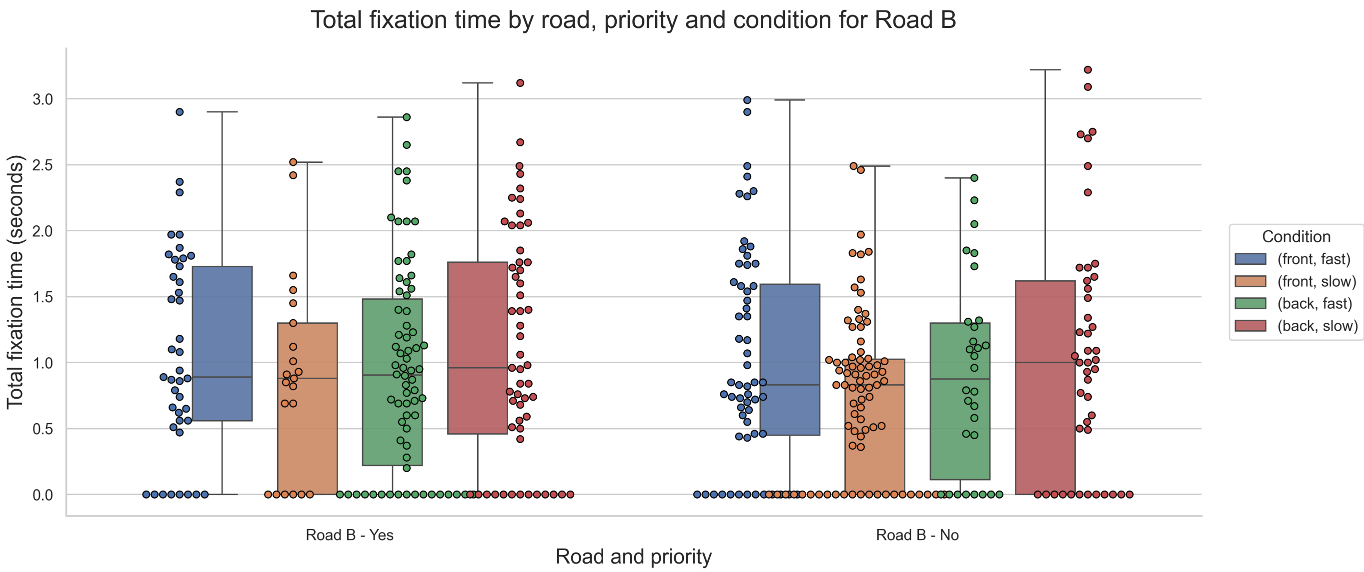

Figure 12: Total fixation time for Road $\mathcal{B}$, grouped by condition and whether the driver went first.

predicting total fixation time, going first did not have a significant effect either ($p = 0.941$). These findings indicate that, within the context of this experiment, gaze behavior measured by fixation count and total fixation duration did not meaningfully differentiate between drivers who yielded and those who proceeded through the roundabout first.

To further explore these results, Figures 11 and 12 break down total fixation time by condition, driver priority and road. These plots focus on combinations of spatial and velocity advantage or disadvantage. Across both Road $\mathcal{A}$ and Road $\mathcal{B}$, slower drivers with a spatial disadvantage often fixated for longer durations, especially when they yielded. These patterns extend the general findings by highlighting how initial conditions shaped visual behavior.

These patterns are supported by the linear mixed-effects models. Table 3 shows that spatial offset had a significant negative effect on total fixation time ($z = -2.304$, $p = 0.0212$), suggesting that drivers positioned further from the intersection fixated for shorter periods. Neither road identity nor velocity offset significantly influenced fixation duration.

In contrast, fixation count showed no significant differences across conditions. Table 4 confirms that neither road identity nor velocity offset significantly predicted the number of fixations. Spatial offset showed a marginal effect ($z = -1.947$, $p = 0.0515$), but did not meet the threshold for significance.

Figures illustrating fixation count for condition, comparable to the fixation time plots shown in Figures 11 and 12, are included in Appendix 4.8. Since no significant effects were found for fixation count, these additional visualizations support transparency but are not central to the main findings.

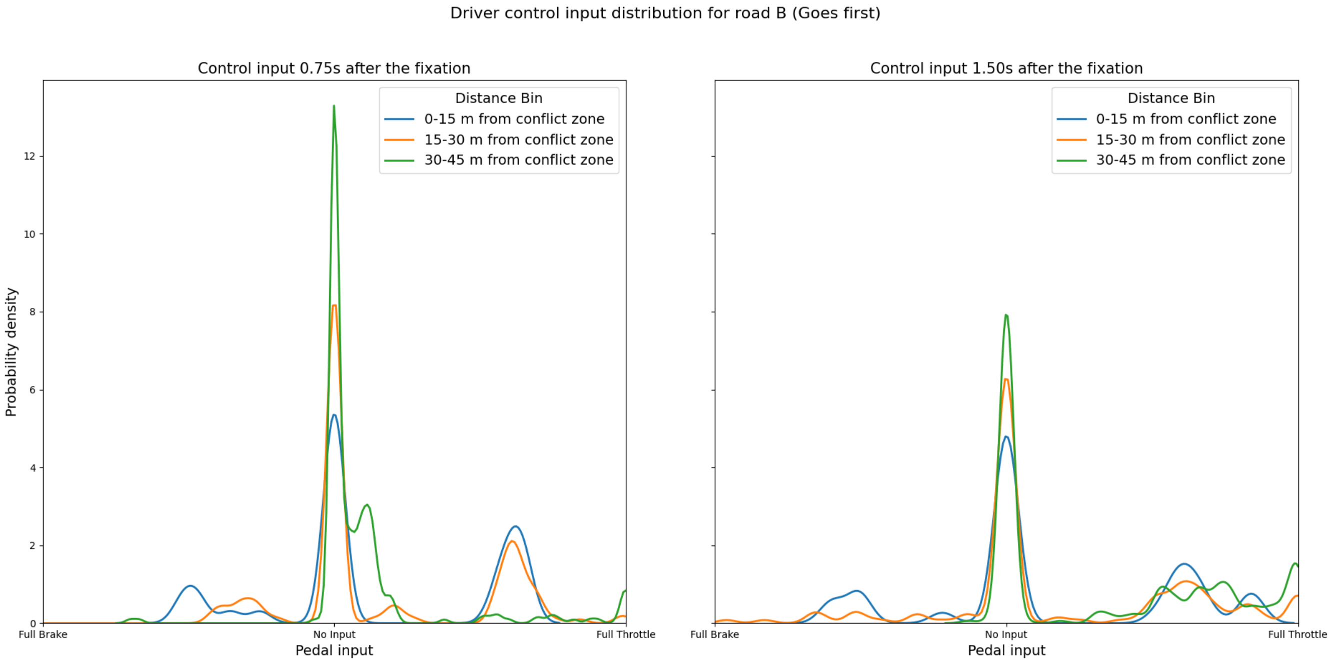

Figure 13: Average input of driver pedal input for drivers on Road $\mathcal{B}$ who proceeded first through the conflict zone. The left panel shows control input 0.75 seconds after the onset of the fixation; the right panel shows input after 1.50 seconds. Pedal input values range from full brake (left) to full throttle (right), with "No Input" at the center. Each line represents a spatial bin based on the driver's distance to the conflict zone at the time of fixation: 0–15 m (blue), 15–30 m (orange) and 30–45 m (green). The y-axis indicates the average driver input, estimated across all drivers and fixations in each condition. A larger version of this figure can be found in Appendix 4.8

Table 3: Results of the Linear Mixed-Effects Model Predicting Total Fixation Time per Trial. The model included spatial offset, velocity offset and Road $\mathcal{A}$'s fixed effects, with a random intercept per participant.

Variable	Estimate	Std. Error	z-value	p-value
Intercept	0.938	0.0690	13.601	< 0.001
Road $\mathcal{B}$	0.022	0.0538	0.409	0.682
Δd	-0.0103	0.0045	-2.304	0.0212
Δv	0.0039	0.0067	0.587	0.557
goes first	0.004	0.058	0.074	0.941
Group Var	0.0571	0.0330	1.730	0.0836

Table 4: Results of the Linear Mixed-Effects Model Predicting Number of Fixations per Trial. The model included spatial offset, velocity offset and Road $\mathcal{A}$'s fixed effects, with a random intercept per participant.

Variable	Estimate	Std. Error	z-value	p-value
Intercept	1.550	0.0567	27.321	< 0.001
Road $\mathcal{B}$	-0.040	0.0565	-0.708	0.479
Δd	-0.0092	0.0047	-1.947	0.0515
Δv	0.0081	0.0071	1.151	0.250
goes first	-0.025	0.061	-0.405	0.685
Group Var	0.0254	0.0180	1.414	0.157

3.3 Driver control input

To investigate how gaze behavior translated into control decisions, we examined the driver's pedal input following gaze fixations. Figure 13 shows the distribution of pedal inputs for drivers on Road $\mathcal{B}$ who proceeded first. The left panel reflects input 0.75 seconds after fixation, while the right panel shows input after 1.5 seconds. Data are grouped into three distance bins from the conflict zone. Drivers at closer distances (0–15 m) responded more decisively, showing a small increase in throttle input and reduced braking compared to the other distances. This pattern suggests a commitment to proceed or brake after fixating on the other vehicle. This is also the case for the median distance (15–30 m). At greater distances, particularly in the 30–45 m range, drivers were more likely to maintain neutral input shortly after fixation, followed by a broader distribution of responses after 1.5 seconds. Likely because of assessing the environment and situation. This shift indicates that initial fixations were followed by a short period of observation before drivers adjusted their behavior. Additional plots for Road $\mathcal{A}$ (both going first and yielding), as well as Road $\mathcal{B}$ yielding, are provided in Appendix 4.8.

3.3.1 Vehicle trajectories

To illustrate how driver interactions unfold during the experiment as a result of the control inputs, Figure 14 presents the vehicle trajectories for a single trial. This is trial 121, which corresponds to the same trial shown in Figures 10 and 9. The plot highlights the trajectories of both vehicles as well as key interaction events such as control handover, mutual visibility and gaze fixations. In this example, Car 1 (from Road $\mathcal{B}$) proceeds through the roundabout first, while Car 2 yields by braking before the yield line. This change in control behavior follows shortly after visual contact between the drivers was established. A contrasting example with the same condition—where Car 2 goes first can be found in Appendix 4.8.

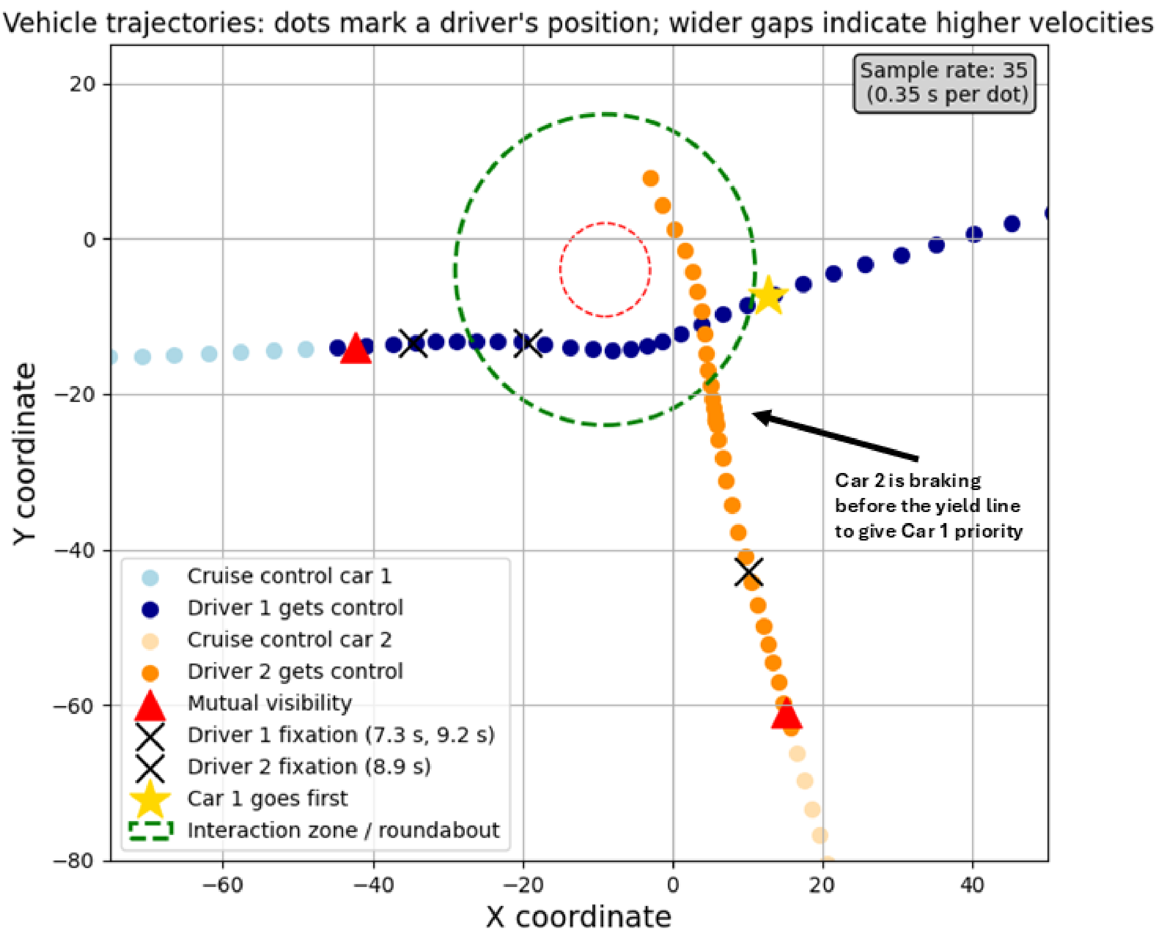

Figure 14: Vehicle trajectories for trial 121, with condition 3. Each dot represents a sampled vehicle position (0.35-second intervals). The blue and orange lines show the trajectories of Car 1 and Car 2, with light segments representing cruise control and dark segments representing manual control. Triangles indicate when mutual visibility occurred, black markers show the fixations and the green dashed circle denotes the interaction zone. The yellow star marks which car entered the conflict zone first. A larger version can be found in Appendix 4.8

4 DISCUSSION

The primary objective of this study was to investigate how human drivers make gap acceptance decisions at roundabouts during mutual interactions. Using a coupled virtual reality driving simulator, we examined which driver proceeded first through the conflict zone and how this outcome related to gaze behavior and control input. Specifically, we quantified the number of fixations and total fixation duration directed precisely at the other vehicle. These gaze metrics, combined with driver control actions following fixation, provided insight into how drivers visually assess the situation and translate this perception into action.

4.1 Driver priority at the conflict zone

The results show that spatial and velocity advantages influenced which driver entered the conflict zone first. Drivers who started closer to the roundabout or had a higher initial velocity were more likely to proceed ahead of the other driver. This outcome shows that drivers used distance and relative speed to evaluate whether they could safely enter the roundabout ahead of the other vehicle.

This behavior aligns with broader findings in the gap acceptance literature, which describe how drivers continuously assess relative speed and distance to determine whether a maneuver is feasible [21]. In roundabout scenarios, this process requires drivers to interpret both the available gap and the potential behavior of nearby vehicles. The current findings support this understanding by showing that the combination of initial position and speed influenced perceived priority.

Studies focused specifically on roundabouts, such as Li et al. [16] and Retting et al. [15], highlight how roundabout geometry and approach speed influence driver decision-making. The spatial and velocity offsets applied in this study reflect these real-world dynamics. The findings offer controlled evidence that, even in a symmetric and simplified roundabout environment, drivers make decisions based on their spatial positioning and motion relative to the other vehicles.

Individual differences may also have contributed to variability in yielding behavior. In some situations, drivers may have chosen to yield despite holding positional advantage, possibly due to differences in confidence, experience or caution.

These insights are particularly relevant for the design of automated systems that must interpret and anticipate human driver behavior at intersections

4.2 Fixation count and total fixation time

This study also examined how gaze behavior varied under different spatial and velocity offsets, with a focus on the number of fixations and the total fixation time directed toward the other vehicle. These gaze metrics offered insight into how drivers monitored and interpreted the behavior of the other road user during the decision-making phase.

The results showed that only spatial offset had a statistically significant effect on gaze behavior. Total fixation time decreased when drivers approached from a longer distance to the yield line, suggesting that proximity to the intersection increased the urgency to observe the other vehicle. No significant effect appeared for fixation count, indicating that drivers did not shift their gaze more frequently, but instead maintained their gaze for a longer period when positioned closer to the intersection. These findings align with prior research showing that drivers allocate more visual attention when the situation involves greater uncertainty or when interactions occur at closer range. For instance, Ma et al. [42] found that closer proximity to conflict points led to longer periods of visual monitoring in driving tasks. The effect of spatial offset on fixation duration reported here supports that interpretation.

More broadly, these findings contribute to ongoing discussions on the role of visual attention in mutual driving interactions. While much of the existing literature has focused on individual gaze behavior in isolated tasks [29, 30], this study considered gaze as a component of continuous mutual adaptation between two drivers. The results support the idea that gaze in these interactions functions not only to gather information but also to regulate coordination by monitoring the other driver's motion and intent [23].

The recent study by Scarí et al. [32] explored this human-human interaction in a dynamic merging scenario using a coupled driving simulator. Their work demonstrated how this setup makes it possible to investigate the mutual behavior between two drivers, particularly under conditions that involve shared gap negotiation. Although their focus was on merging and this study examined roundabout entry, both scenarios required drivers to assess gaps and monitor the behavior of another vehicle.

These findings contribute to the broader literature on human-human decision-making in traffic. While traditional models treat gap acceptance as an individual, instantaneous process [19, 20], the results underscore the mutual nature of driver interaction. Gaze behavior reflects this ongoing monitoring, although it does not directly predict which driver proceeds first. Instead, gaze serves as part of a larger, adaptive process shaped by timing, control input and spatial context. Total fixation time, rather than fixation count, proved to be the more informative metric, offering insight into how drivers regulate their attention during these interactions.

4.3 Control input

The control input data provide additional insight into how drivers translated visual monitoring into action. Drivers who were closer to the conflict zone at the time of fixation often responded quickly with a clear control decision, such as acceleration or braking. In contrast, drivers at greater distances showed more variability and introduced delays in their responses. These results suggest a close temporal link between gaze behavior and control input in situations where time pressure was higher due to proximity.

Gaze fixations did not reflect passive observation but appeared to trigger immediate behavioral adjustments. This pattern points to a strong coupling between perception and control during interactions at roundabouts. These findings underscore the need to account for gaze-driven control behavior when designing AV systems for environments that demand rapid mutual decision-making, such as roundabouts.

4.4 Limitations

This study has several limitations that should be considered when interpreting the results. The first limitation is the small sample size. The data of five experiments or ten participants was included in the final analysis. Halfway through the experiment, an error was discovered in the implementation of the experimental conditions. As a result, half of the data had to be discarded. This reduced the statistical power of the study and may have influenced the final outcomes. A larger sample size, ideally with at least twenty or more participants, would have provided more robust and generalizable results.

The participant pool consisted of students and researchers affiliated with TU Delft. Their average age was 23.6 years (SD = 3.0 years). This narrow demographic may not be fully representative of the general driving population. Additionally, as participants were affiliated with a technical university, they may have been more familiar with automated driving technologies, which could have influenced their behavior in the simulation.

Another limitation relates to the use of a virtual reality headset. Wearing a VR headset introduced minor physical discomfort for some participants, especially during the final trials. This discomfort may have limited head movements, particularly toward the end of the experiment when fatigue likely increased. Reduced head movement may have influenced the gaze data, particularly the fixation measures. This limitation is critical, as the study aimed to determine whether participants directed their gaze precisely at the other vehicle. However, participants may have relied more on eye movements and specifically their peripheral vision, rather than turning their heads, to observe the other driver.

Another limitation concerns the realism of the simulation and participant engagement. Participants knew beforehand they would always interact with the same other driver. Although this did not affect early trials, repeated exposure to the experimental conditions may have influenced behavior. Anticipating the actions of the other driver does not reflect the uncertainty found in real traffic. Additionally, the absence of real-world consequences such as injury or vehicle damage may have encouraged more aggressive or risk-tolerant decisions. The environment was also highly simplified, with only two vehicles, no other traffic, no pedestrians and no external distractions such as signage or weather. Participants also faced no time constraints or secondary tasks, which reduced cognitive load. While the controlled setup focused on specific variables like gaze and decision-making, it did not reflect the full range of challenges drivers face in real traffic conditions.

The virtual environment also introduced challenges in accurately replicating longitudinal vehicle dynamics. Participants often underestimated their velocity, believing they were driving slower than they actually were. This mismatch caused some participants to accelerate more often when circulating within the roundabout. Such behavior altered the interaction dynamics and would likely not occur in real driving scenarios.

Finally, the lack of prior research on human-human interactions at roundabouts is another limitation. Existing studies have primarily focused on individual driver behavior or interactions with automated vehicles. As a result, little empirical data exists on how two human drivers respond to each other in roundabout scenarios. This limited reference base makes it difficult to compare the current findings to established patterns or to validate the experimental setup against real-world observations.

4.5 Future works

Future studies should include a larger and more diverse participant sample to improve the generalizability of the findings. Participants with varying driving experience and a broader age range would allow for analysis of how individual differences affect gaze behavior and gap acceptance at roundabouts.

Future studies should also increase the complexity of the simulation environment. Adding other vehicles, pedestrians, road signage and varying weather conditions would help capture how drivers adapt to more realistic and dynamic traffic situations. Introducing time constraints or secondary tasks would reflect real-world cognitive load, which may influence both gaze patterns and decision-making.

Future studies should compare human-human interactions with human-autonomous interactions in similar roundabout scenarios. This would provide insights into how the presence of autonomous vehicles affects mutual decision-making and visual attention. The role of explicit communication cues, such as turn indicators or vehicle positioning, should also be explored as these were not applied during this study.

Finally, future studies should improve the accuracy of perceived speed and vehicle dynamics in virtual environments. More realistic feedback would ensure that observed behaviors closely reflect real-world driving and support the development of better human-human driver behavior models.

4.6 Conclusions

In this study, we analyzed the interaction dynamics between two human drivers during roundabout approach and entry scenarios. This was done by evaluating the outcome of driver priority at the conflict zone the corresponding gaze behavior and control inputs. Based on the experimental conditions and statistical analyses, we assessed and concluded the following:

1) Drivers who approached from a shorter distance or at a higher velocity were more likely to proceed first through the roundabout.
2) Drivers fixated longer on the other vehicle when they were closer to the conflict zone.
3) Fixation count remained stable across conditions, suggesting that gaze duration rather than frequency—reflected engagement in the interaction.
4) Gaze behavior alone did not predict who proceeded first, implying that mutual decisions emerged from a broader set of factors beyond eye movements.
5) Drivers closer to the conflict zone responded more decisively after fixating by pressing the gas or brake pedal compared to drivers further away from the conflict zone.

These findings highlight the value of incorporating human factors, such as visual attention and decision-making cues, into the design and evaluation of autonomous vehicles to support their integration into real traffic environments. Insights into human gaze behavior and gap acceptance can help ensure that AVs respond in ways that match driver expectations. This can support safer and more intuitive interactions between AVs and human drivers.

4.7 Acknowledgments

We would like to thank Arkady Zgonnikov for the valuable discussions, insightful suggestions and support throughout the project. We would also like to thank Federico Scarí for his support during the entire project. This includes but is not limited to experiment development, execution and technical support for CARLA and JOAN.

4.8 Declaration of AI assistance in writing

During the preparation of this work, we used OpenAI's ChatGPT for grammar refinement, typo correction and terminology adjustments. The tool was not used to generate content. Following its use, we carefully reviewed and edited the material as necessary and assume full responsibility for the final content.

References

[1] Dimitris Milakis, Bart Van Arem, and Bert Van Wee. "Policy and society related implications of automated driving: A review of literature and directions for future research". In: *Journal of intelligent transportation systems* 21.4 (2017), pp. 324–348.

[2] Peter A Hancock, Illah Nourbakhsh, and Jack Stewart. "On the future of transportation in an era of automated and autonomous vehicles". In: *Proceedings of the National Academy of Sciences* 116.16 (2019), pp. 7684–7691.

[3] Monika Stoma et al. "The future of autonomous vehicles in the opinion of automotive market users". In: *Energies* 14.16 (2021), p. 4777.

[4] Darsh Parekh et al. "A review on autonomous vehicles: Progress, methods and challenges". In: *Electronics* 11.14 (2022), p. 2162.

[5] Todd Litman. "Autonomous vehicle implementation predictions". In: (2017).

[6] Amit Chougule et al. "A comprehensive review on limitations of autonomous driving and its impact on accidents and collisions". In: *IEEE Open Journal of Vehicular Technology* 5 (2023), pp. 142–161.

[7] Safe Autonomy. *A Reality Check on the 94 Percent Human Error Statistic for Automated Cars*. Accessed: 2024-10-10. 2018. URL: https://safeautonomy.blogspot.com/2018/06/a-reality-check-on-94-percent-human.html.

[8] Ken Allen Law. *Myth That Driver Error Causes 94% of Car Crashes: The Complexities of Motor Vehicle Accident Causation*. May 2024. URL: https://www.kenallenlaw.com/2024/05/myth-that-driver-error-causes-94-of-car-crashes-the-complexities-of-motor-vehicle-accident-causation/.

[9] Ramin Arvin et al. "Safety evaluation of connected and automated vehicles in mixed traffic with conventional vehicles at intersections". In: *Journal of Intelligent Transportation Systems* 25.2 (2020), pp. 170–187.

[10] Wilko Schwarting et al. "Social behavior for autonomous vehicles". In: *Proceedings of the National Academy of Sciences* 116.50 (2019), pp. 24972–24978.

[11] Hananeh Alambeigi, Anthony D McDonald, and Srinivas R Tankasala. "Crash themes in automated vehicles: A topic modeling analysis of the California Department of Motor Vehicles automated vehicle crash database". In: *arXiv preprint arXiv:2001.11087* (2020).

[12] Wilbert Tabone et al. "Vulnerable road users and the coming wave of automated vehicles: Expert perspectives". In: *Transportation research interdisciplinary perspectives* 9 (2021), p. 100293.

[13] Elżbieta Macioszek. "Roundabouts as aesthetic road solutions for organizing landscapes". In: *Zeszyty Naukowe. Transport/Politechnika Śląska* (2022).

[14] Antonio Pratelli et al. "Mini-roundabouts for improving urban accessibility". In: *Modelling of the Interaction of the Different Vehicles and Various Transport Modes* (2020), pp. 333–382.

[15] Richard A Retting et al. "Crash and injury reduction following installation of roundabouts in the United States". In: *American journal of public health* 91.4 (2001), p. 628.

[16] Li Li et al. "The role of traffic conflicts in roundabout safety evaluation: A review". In: *Accident Analysis & Prevention* 196 (2024), p. 107430.

[17] Ali Danesh et al. "Optimal roundabout control under fully connected and automated vehicle environment". In: *IET Intelligent Transport Systems* 15.11 (2021), pp. 1440–1453.

[18] Marilo Martin-Gasulla and Lily Elefteriadou. "Single-lane roundabout manager under fully automated vehicle environment". In: *Transportation research record* 2673.8 (2019), pp. 439–449.

[19] Oriol Pascual Anglès et al. "Gap-acceptance Behavior and Safety Analysis in Roundabouts". In: *104th Annual Meeting of the Transportation Research Board*. 2025.

[20] Arkady Zgonnikov, David Abbink, and Gustav Markkula. "Should I stay or should I go? Cognitive modeling of left-turn gap acceptance decisions in human drivers". In: *Human factors* 66.5 (2024), pp. 1399–1413.

[21] Jason Dahl and Chris Lee. "Empirical estimation of capacity for roundabouts using adjusted gap-acceptance parameters for trucks". In: *Transportation research record* 2312.1 (2012), pp. 34–45.

[22] Manish Dutta and Mokaddes Ali Ahmed. "Gap acceptance behavior of drivers at uncontrolled T-intersections under mixed traffic conditions". In: *Journal of modern transportation* 26.2 (2018), pp. 119–132.

[23] Gustav Markkula et al. "Defining interactions: A conceptual framework for understanding interactive behaviour in human and automated road traffic". In: *Theoretical Issues in Ergonomics Science* 21.6 (2020), pp. 728–752.

[24] Anirudh Sripada, Pavlo Bazilinskyy, and Joost de Winter. "Automated vehicles that communicate implicitly: examining the use of lateral position within the lane". In: *Ergonomics* 64.11 (2021), pp. 1416–1428.

[25] Evangelia Portouli, Dimitris Nathanael, and Nicolas Marmaras. "Drivers' communicative interactions: on-road observations and modelling for integration in future automation systems". In: *Ergonomics* 57.12 (2014), pp. 1795–1805.

[26] Jennifer Sudkamp, Mateusz Bocian, and David Souto. "The role of eye movements in perceiving vehicle speed and time-to-arrival at the roadside". In: *Scientific reports* 11.1 (2021), p. 23312.

[27] Luiz Gustavo Buzon et al. "Effect of speed on driver's visual attention: a study using a driving simulator". In: *Transportation in developing economies* 8 (2021), pp. 1–11.

[28] Zengke Qin et al. "Analysis of Driver Gaze Behaviors at Curve of Secondary Highway with Different Driving Speeds". In: *CICTP 2020*. 2020, pp. 665–675.

[29] Sophie Lemonnier, Roland Brémond, and Thierry Baccino. "Gaze behavior when approaching an intersection: Dwell time distribution and comparison with a quantitative prediction". In: *Transportation research part F: traffic psychology and behaviour* 35 (2015), pp. 60–74.

[30] MP Hagenzieker. "Eye movements in traffic safety research". In: *Paper Third Intemational Conference on VisuaI Search*. 1992.

[31] Elena Campi et al. "Roundabouts: Traffic simulations of connected and automated vehicles—a state of the art". In: *IEEE Transactions on Intelligent Transportation Systems* 25.5 (2023), pp. 3305–3325.

[32] Federico Scarí. "An Evaluation of the Merging Interaction between Humans and Interaction-Aware Vehicles". Mentor: O. Siebinga, Committee Member: A. Zgonnikov. Master's Thesis. Delft, Netherlands: Delft University of Technology, 2024. URL: https://repository.tudelft.nl/record/uuid:a11ad2df-5f5e-4bb4-a335-596e8d35817f.

[33] Michel Wedel, Rik Pieters, and Ralf van der Lans. "Modeling eye movements during decision making: A review". In: *psychometrika* 88.2 (2023), pp. 697–729.

[34] Alexey Dosovitskiy et al. "CARLA: An Open Urban Driving Simulator". In: *Proceedings of the 1st Annual Conference on Robot Learning*. Vol. 78. PMLR, 2017, pp. 1–16.

[35] Advait Valluri. *Automated Driving in the Urban Environment with RoadRunner Scenario*. MathWorks Automotive Conference 2024 Europe. June 2024. URL: https://de.mathworks.com/videos/automated-

driving-in-the-urban-environment-with-roadrunner-scenario-1717504404725.html.

[36] Niek Beckers et al. "JOAN: a framework for human-automated vehicle interaction experiments in a virtual reality driving simulator". In: *Journal of Open Source Software* 8.82 (2023), p. 4250. DOI: 10.21105/joss.04250. URL: https://doi.org/10.21105/joss.04250.

[37] Abhijat Biswas and Henny Admoni. "Characterizing Drivers' Peripheral Vision via the Functional Field of View for Intelligent Driving Assistance". In: *2023 IEEE Intelligent Vehicles Symposium (IV)*. 2023, pp. 1–8. DOI: 10.1109/IV55152.2023.10186746.

[38] Kristián Čulík, Alica Kalašová, and Vladimíra Štefancová. "Evaluation of driver's reaction time measured in driving simulator". In: *Sensors* 22.9 (2022), p. 3542.

[39] Robert Stojan et al. "Effect of additional tasks on the reaction time of braking responses in simulated car driving: beyond the PRP effect". In: *Psychological research* 88.7 (2024), pp. 2096–2106.

[40] Eshin Jolly. "Pymer4: Connecting R and Python for linear mixed modeling". In: *Journal of Open Source Software* 3.31 (2018), p. 862.

[41] Skipper Seabold and Josef Perktold. "Statsmodels: Econometric and statistical modeling with python". In: *9th Python in Science Conference*. 2010.

[42] Yanli Ma et al. "Drivers' visual attention characteristics under different cognitive workloads: An on-road driving behavior study". In: *International journal of environmental research and public health* 17.15 (2020), p. 5366.

Appendix A: Number of fixations by road, priority and condition

Appendix A shows the number of fixations made by drivers toward the other vehicle. The data is grouped by whether the driver went first through the conflict zone and by experimental conditions. The box plots below display the fixation counts for Road $\mathcal{A}$ and Road $\mathcal{B}$. Each colored bar corresponds to a different combination of spatial and velocity offset. The results show that fixation count stayed relatively stable across all conditions, with only minor variation between drivers who went first and those who yielded.

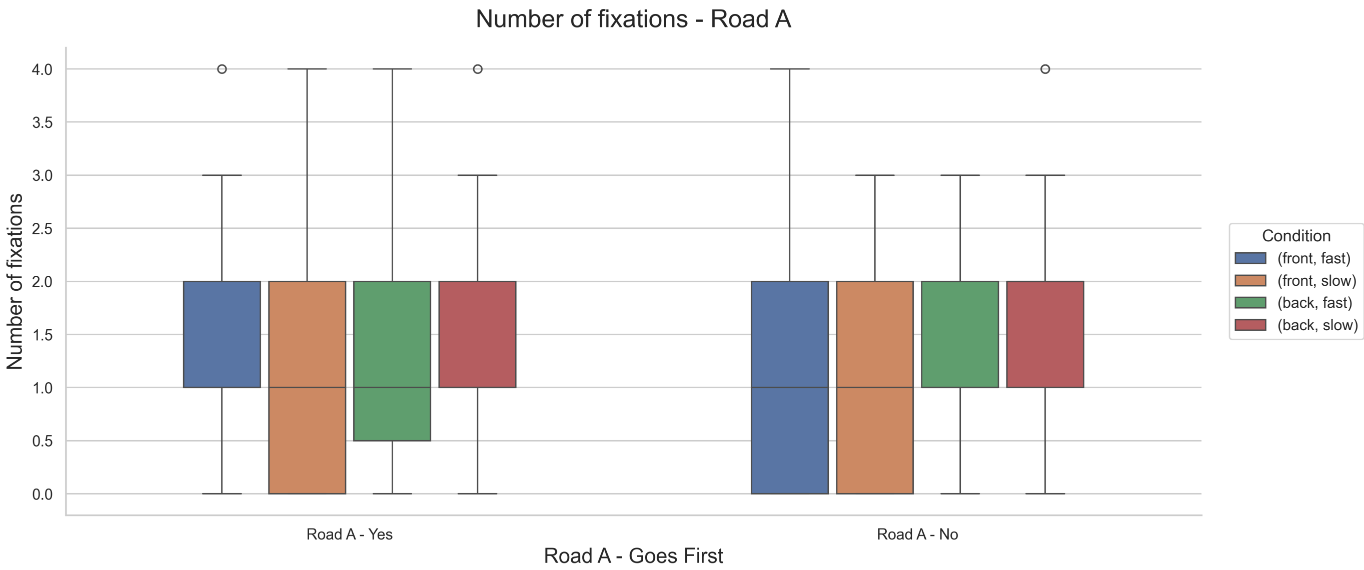

Figure 15: Number of fixations for Road $\mathcal{A}$ drivers, grouped by whether the driver went first and by condition.

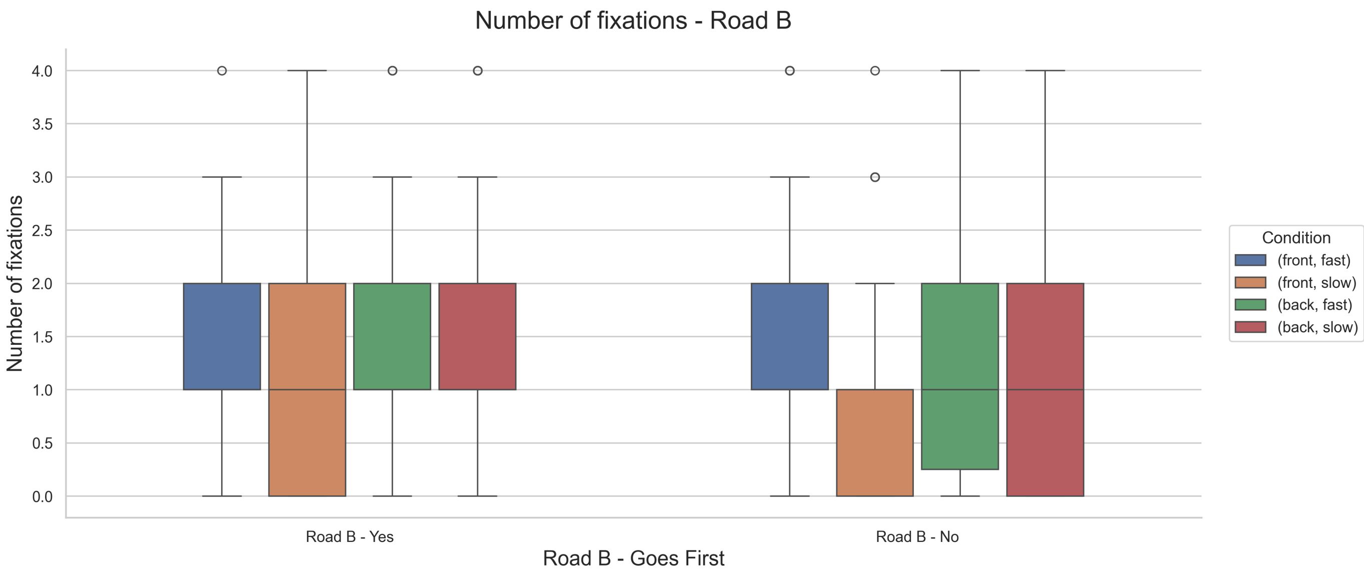

Figure 16: Number of fixations for Road $\mathcal{B}$ drivers, grouped by whether the driver went first and by condition.

APPENDIX B: CONTROL INPUTS

Appendix B presents the distribution of driver pedal inputs after gaze fixations, separated by road, priority and distance to the conflict zone. The figures compare average control behavior for drivers who either proceeded first or yielded. Each plot distinguishes between three distance bins at the moment of fixation: 0–15 m, 15–30 m and 30–45 m from the conflict zone. The left panels show control input 0.75 seconds after the start of the fixation; the right panels show input 1.50 seconds after. These distributions provide insight into how gaze was followed by throttle or brake responses under different spatial conditions.

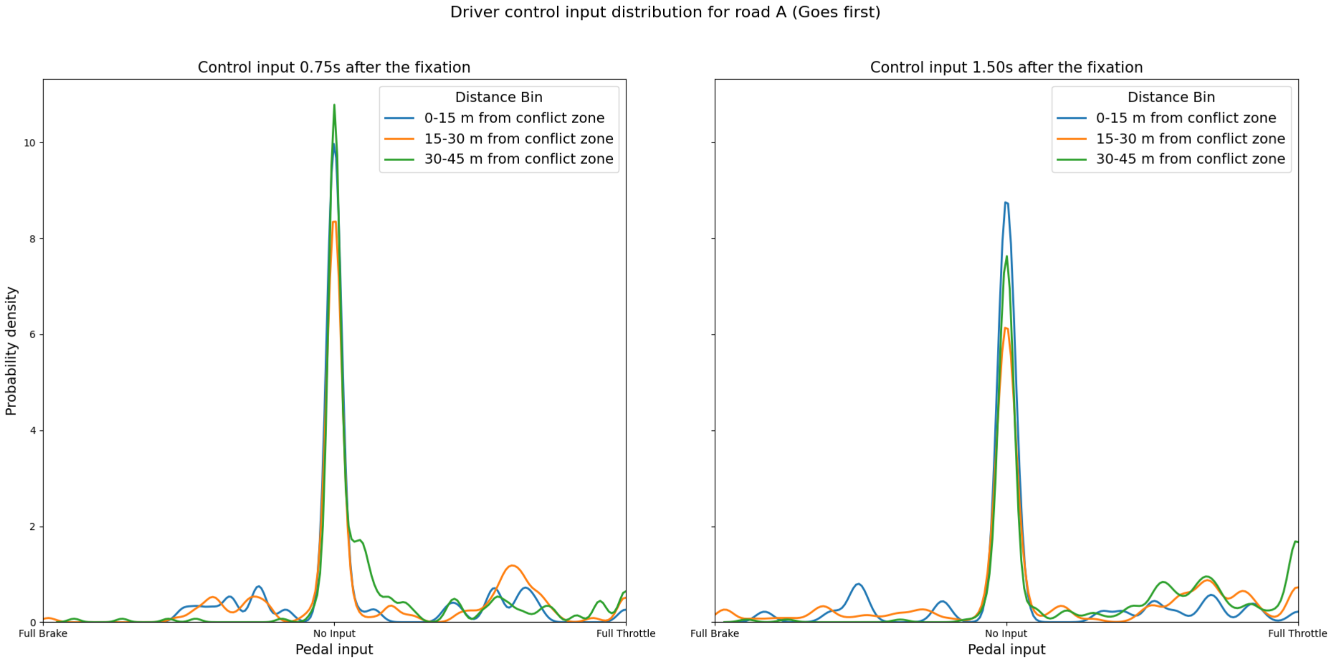

Figure 17: Average pedal input for drivers on Road $\mathcal{A}$ who proceeded first through the conflict zone. The left panel shows input 0.75 seconds after fixation onset; the right panel shows input 1.50 seconds after. Each line reflects a distance bin at the time of fixation: 0–15 m (blue), 15–30 m (orange) and 30–45 m (green). The y-axis shows the average driver control input.

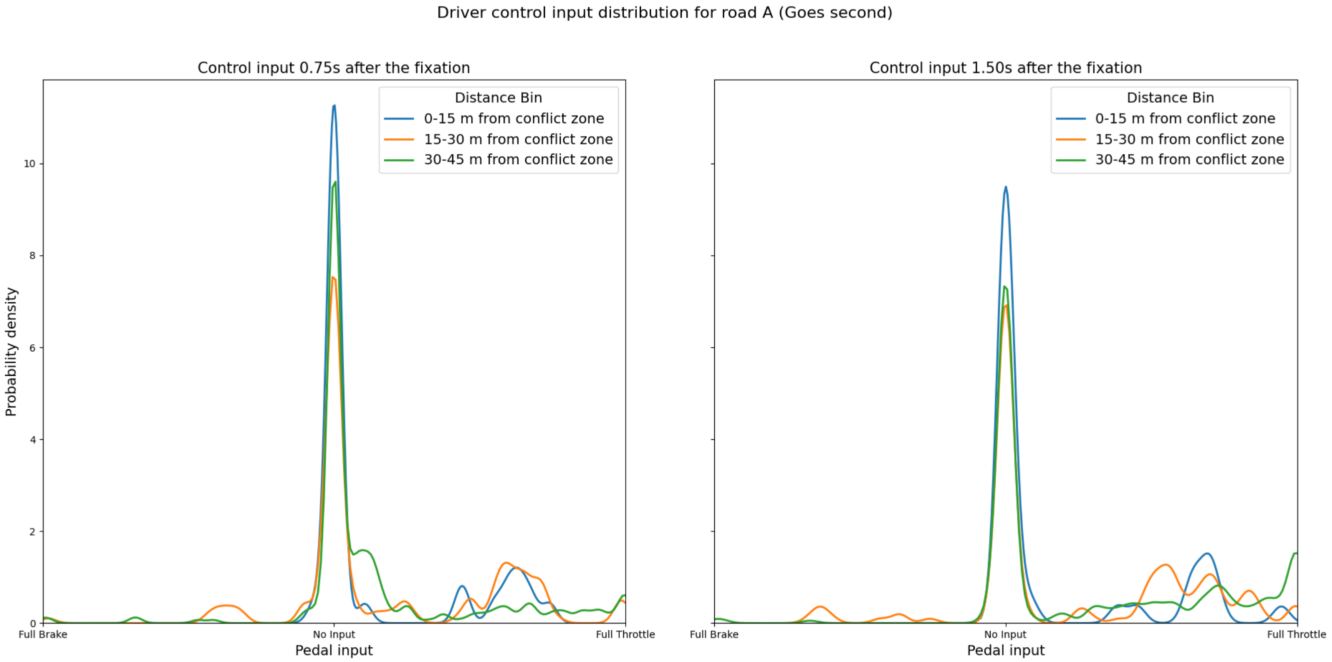

Figure 18: Average pedal input for drivers on Road $\mathcal{A}$ who yielded at the conflict zone. The left panel shows input 0.75 seconds after fixation onset; the right panel shows input 1.50 seconds after. Each line reflects a distance bin at the time of fixation: 0–15 m (blue), 15–30 m (orange) and 30–45 m (green). The y-axis shows the average driver control input.

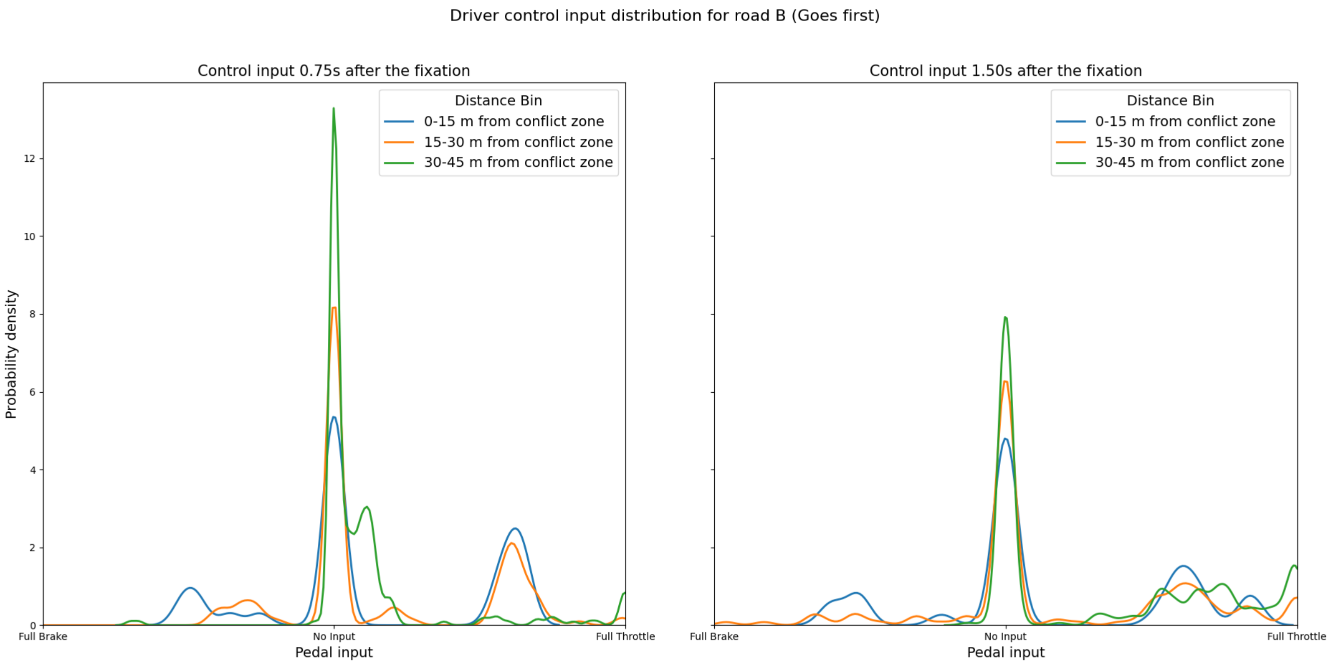

Figure 19: Average pedal input for drivers on Road $\mathcal{B}$ who proceeded first through the conflict zone. The left panel shows input 0.75 seconds after fixation onset; the right panel shows input 1.50 seconds after. Each line reflects a distance bin at the time of fixation: 0–15 m (blue), 15–30 m (orange) and 30–45 m (green). The y-axis shows the average driver control input.

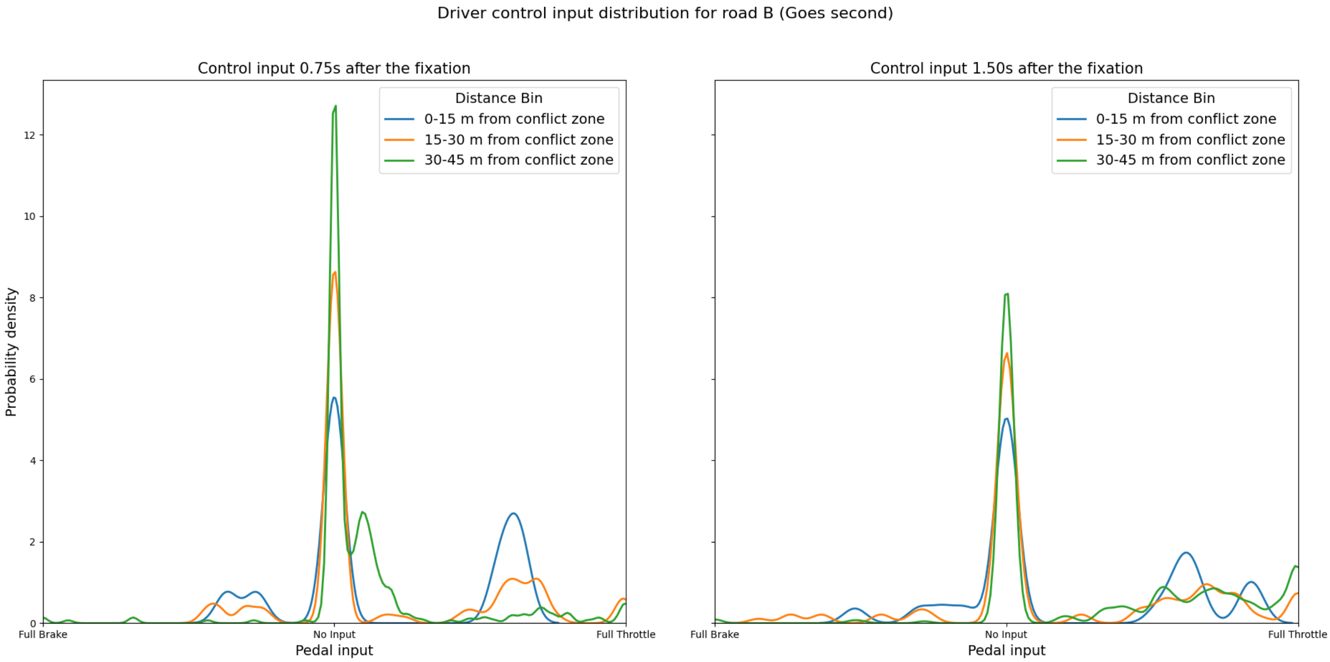

Figure 20: Average pedal input for drivers on Road $\mathcal{B}$ who yielded at the conflict zone. The left panel shows input 0.75 seconds after fixation onset; the right panel shows input 1.50 seconds after. Each line reflects a distance bin at the time of fixation: 0–15 m (blue), 15–30 m (orange) and 30–45 m (green). The y-axis shows the average driver control input.

APPENDIX B.2: CONTROL INPUT HISTOGRAMS BY CONDITION

This section presents a series of histograms that show the distribution of normalized control inputs—throttle and brake—for all experimental conditions. Each figure corresponds to one of the eight condition pairs defined by initial vehicle position (front/back) and speed (fast/slow), observed separately for drivers on Road $\mathcal{A}$ and Road $\mathcal{B}$. For each condition, the control input is shown for trials where the driver went first (green) and where the driver yielded (red). These distributions provide insight into how control behavior differed based on the driver's spatial position, approach speed, and whether they claimed priority at the roundabout.

The opposing condition is included in each figure for comparison. For example, when Road $\mathcal{A}$ is back and fast, the corresponding Road $\mathcal{B}$ condition is front and slow. This pairing allows a side-by-side interpretation of how drivers from both directions behaved in scenarios with the same relative geometry but different outcomes.

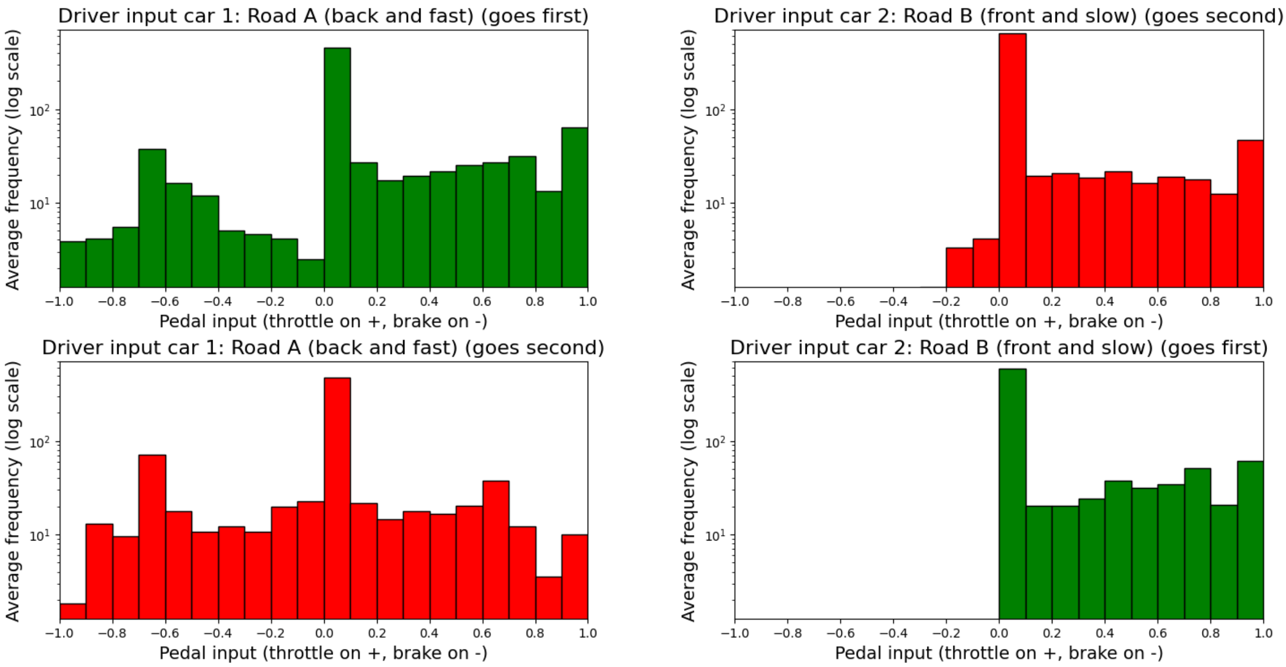

Figure 21: Average control input distribution for the condition where Car 1 on Road $\mathcal{A}$ starts *back and fast*. The x-axis represents normalized pedal input, with positive values indicating throttle and negative values indicating braking. The y-axis shows average frequency on a logarithmic scale. The top left plot shows control input for Car 1 when it goes first (green), and the bottom left shows the same condition when Car 1 goes second (red). The right plots show the opposite condition—Car 2 on Road $\mathcal{B}$ starting *front and slow*. In the top right, Car 2 goes second (red), and in the bottom right, it goes first (green).

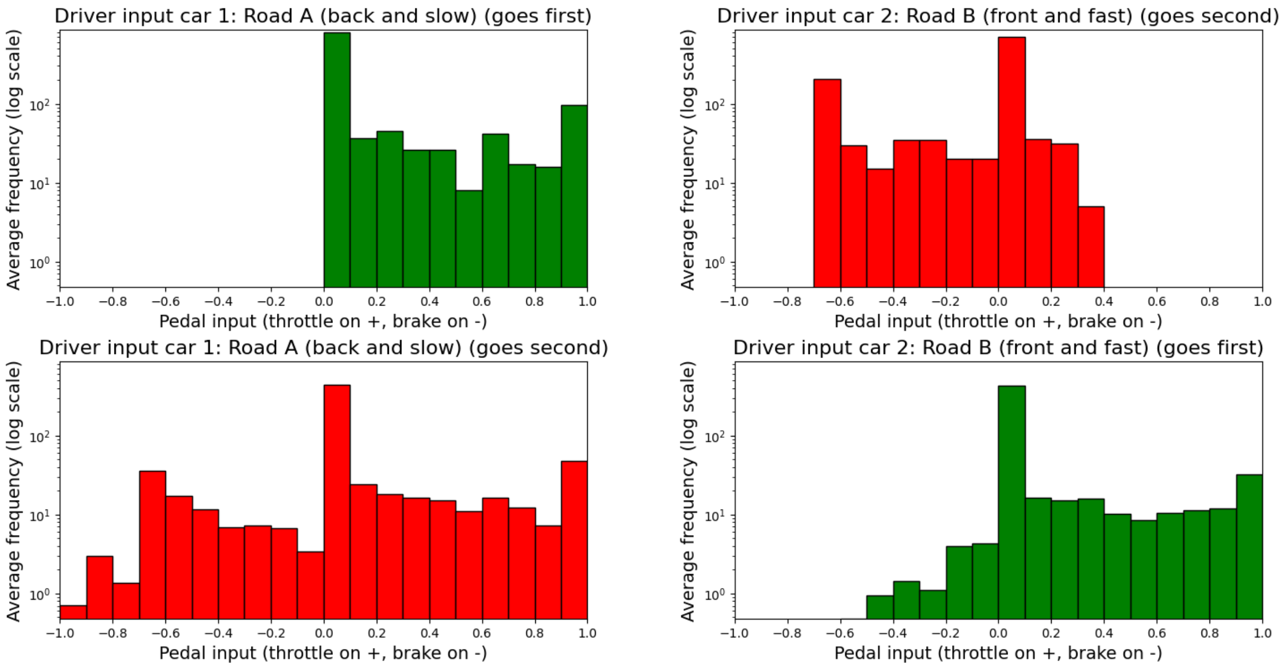

Figure 22: Average control input distribution for the condition where Car 1 on Road $\mathcal{A}$ starts *back and slow*. TThe x-axis represents normalized pedal input, with positive values indicating throttle and negative values indicating braking. The y-axis shows average frequency on a logarithmic scale. The top left plot shows input for Car 1 when it goes first (green), and the bottom left shows the same condition when Car 1 goes second (red). The right side reflects the opposite condition—Car 2 on Road $\mathcal{B}$ starts *front and fast*. The top right shows Car 2 when yielding (red), and the bottom right when going first (green).

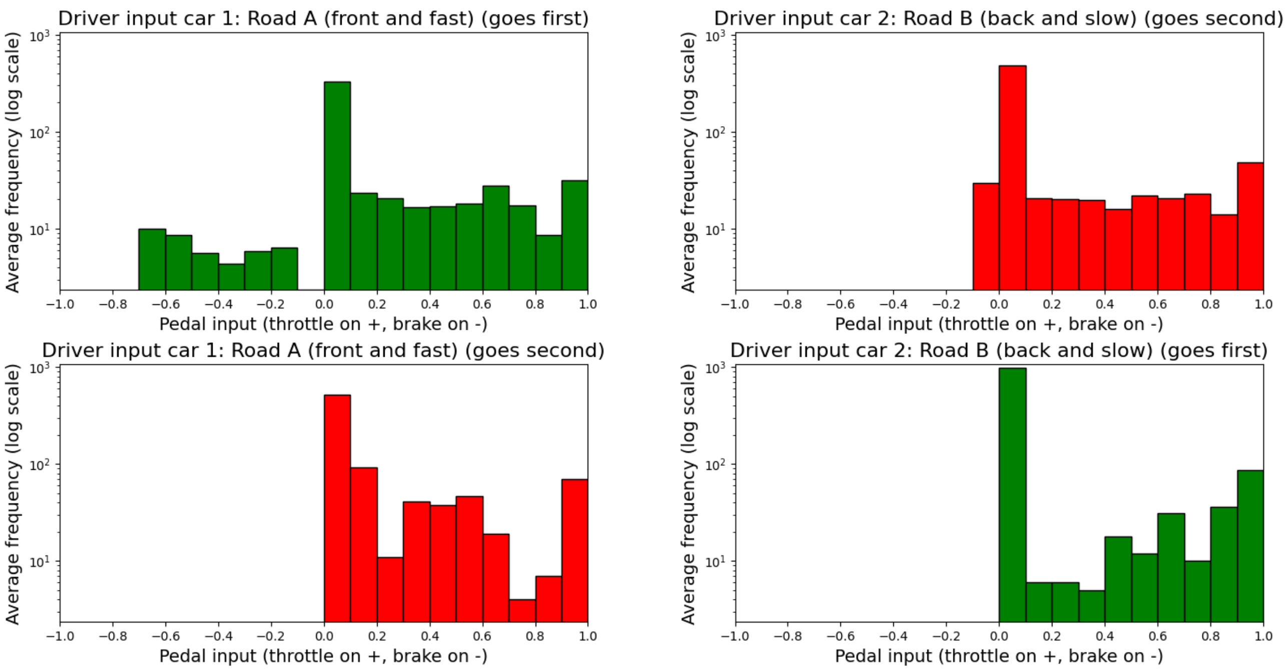

Figure 23: Average control input distribution for the condition where Car 1 on Road $\mathcal{A}$ starts *front and fast*. The x-axis represents normalized pedal input, with positive values indicating throttle and negative values indicating braking. The y-axis shows average frequency on a logarithmic scale. The top left plot shows input for Car 1 when it goes first (green), and the bottom left shows the same condition when Car 1 goes second (red). The right side reflects the opposite condition—Car 2 on Road $\mathcal{B}$ starts *back and slow*. The top right shows Car 2 when yielding (red), and the bottom right when going first (green).

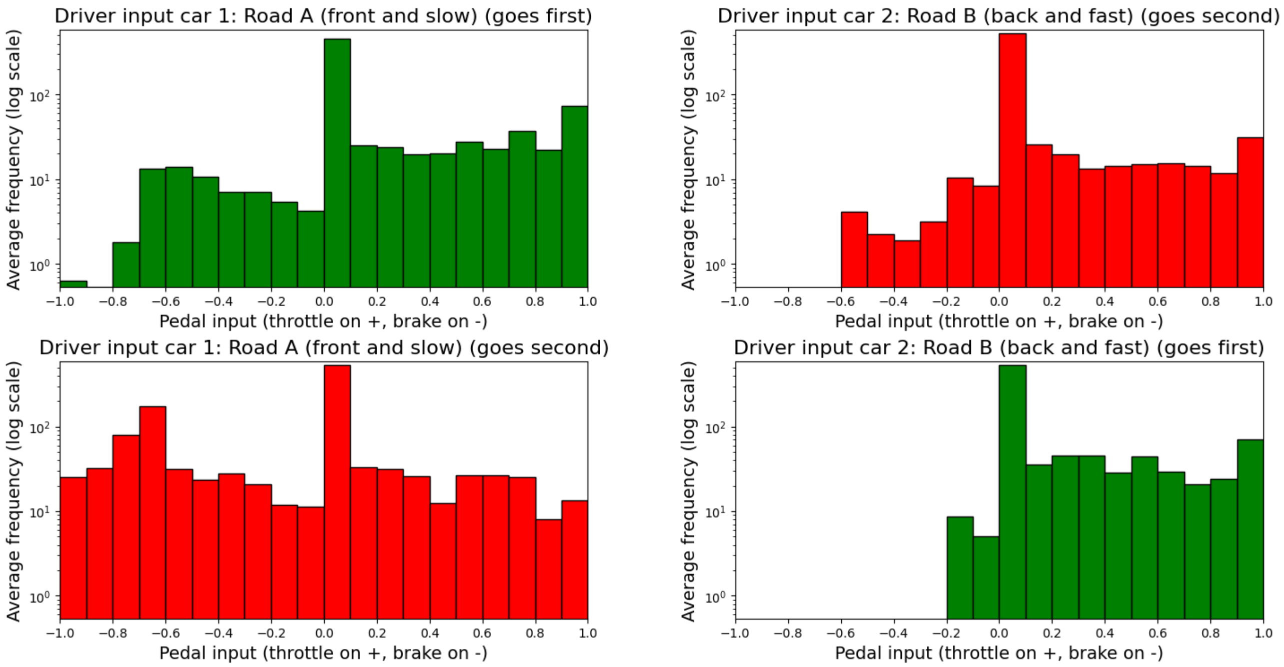

Figure 24: Average control input distribution for the condition where Car 1 on Road $\mathcal{A}$ starts *front and slow*. The x-axis represents normalized pedal input, with positive values indicating throttle and negative values indicating braking. The y-axis shows average frequency on a logarithmic scale. The top left plot shows input for Car 1 when it goes first (green), and the bottom left shows the same condition when Car 1 goes second (red). The right side reflects the opposite condition—Car 2 on Road $\mathcal{B}$ starts *back and fast*. The top right shows Car 2 when yielding (red), and the bottom right when going first (green).

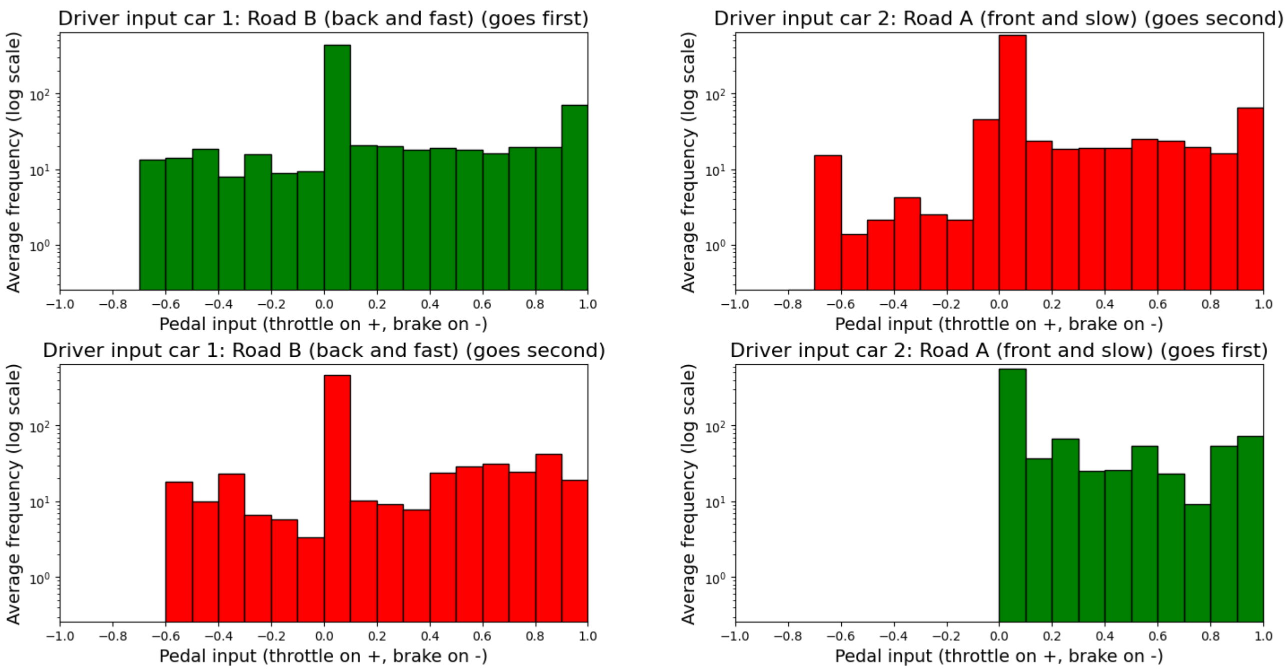

Figure 25: Average control input distribution for the condition where Car 1 on Road $\mathcal{B}$ starts *back and fast*. The x-axis represents normalized pedal input, with positive values indicating throttle and negative values indicating braking. The y-axis shows average frequency on a logarithmic scale. The top left plot shows input for Car 1 when it goes first (green), and the bottom left shows the same condition when Car 1 goes second (red). The right side reflects the opposite condition—Car 2 on Road $\mathcal{A}$ starts *front and slow*. The top right shows Car 2 when yielding (red), and the bottom right when going first (green).

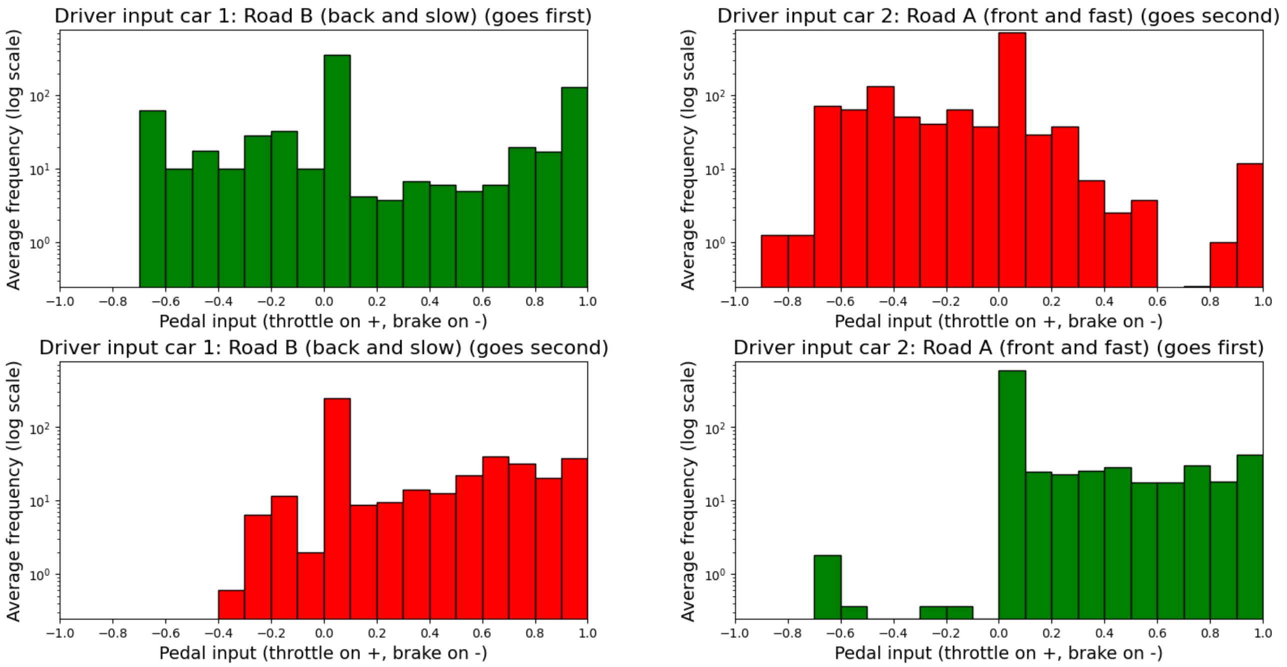

Figure 26: Average control input distribution for the condition where Car 1 on Road $\mathcal{B}$ starts *back and slow*. The x-axis represents normalized pedal input, with positive values indicating throttle and negative values indicating braking. The y-axis shows average frequency on a logarithmic scale. The top left plot shows input for Car 1 when it goes first (green), and the bottom left shows the same condition when Car 1 goes second (red). The right side reflects the opposite condition—Car 2 on Road $\mathcal{A}$ starts *front and fast*. The top right shows Car 2 when yielding (red), and the bottom right when going first (green).

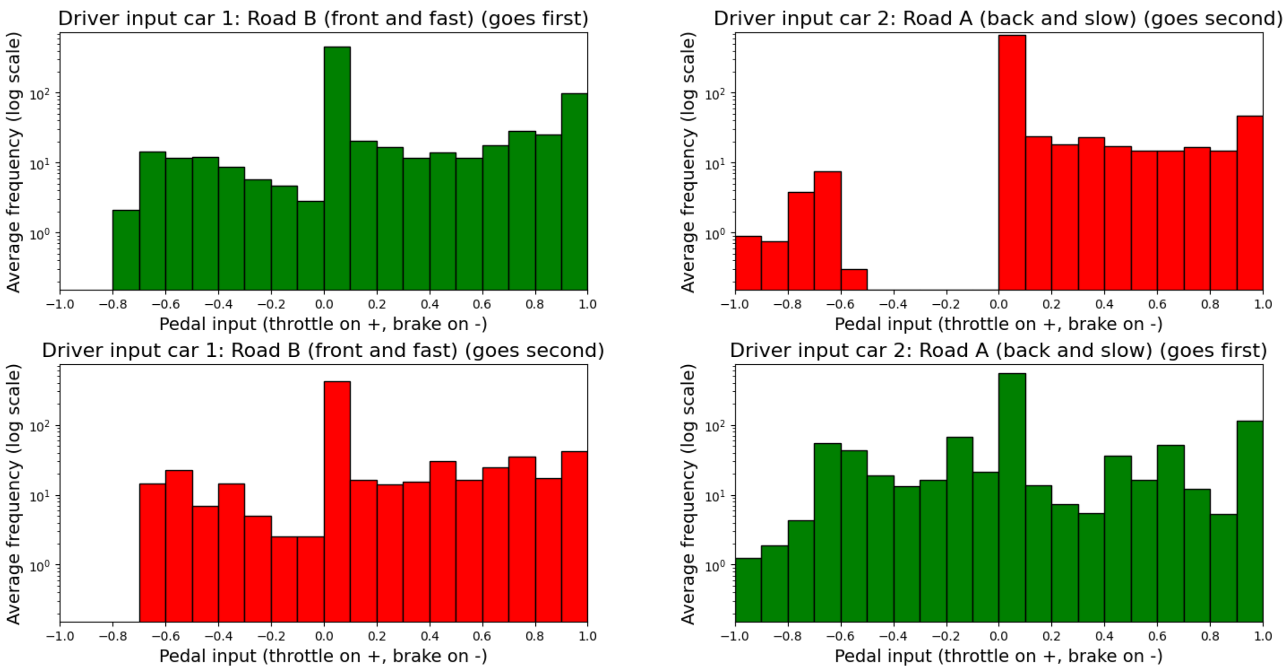

Figure 27: Average control input distribution for the condition where Car 1 on Road $\mathcal{B}$ starts *front and fast*. The x-axis represents normalized pedal input, with positive values indicating throttle and negative values indicating braking. The y-axis shows average frequency on a logarithmic scale. The top left plot shows input for Car 1 when it goes first (green), and the bottom left shows the same condition when Car 1 goes second (red). The right side reflects the opposite condition—Car 2 on Road $\mathcal{A}$ starts *back and slow*. The top right shows Car 2 when yielding (red), and the bottom right when going first (green).

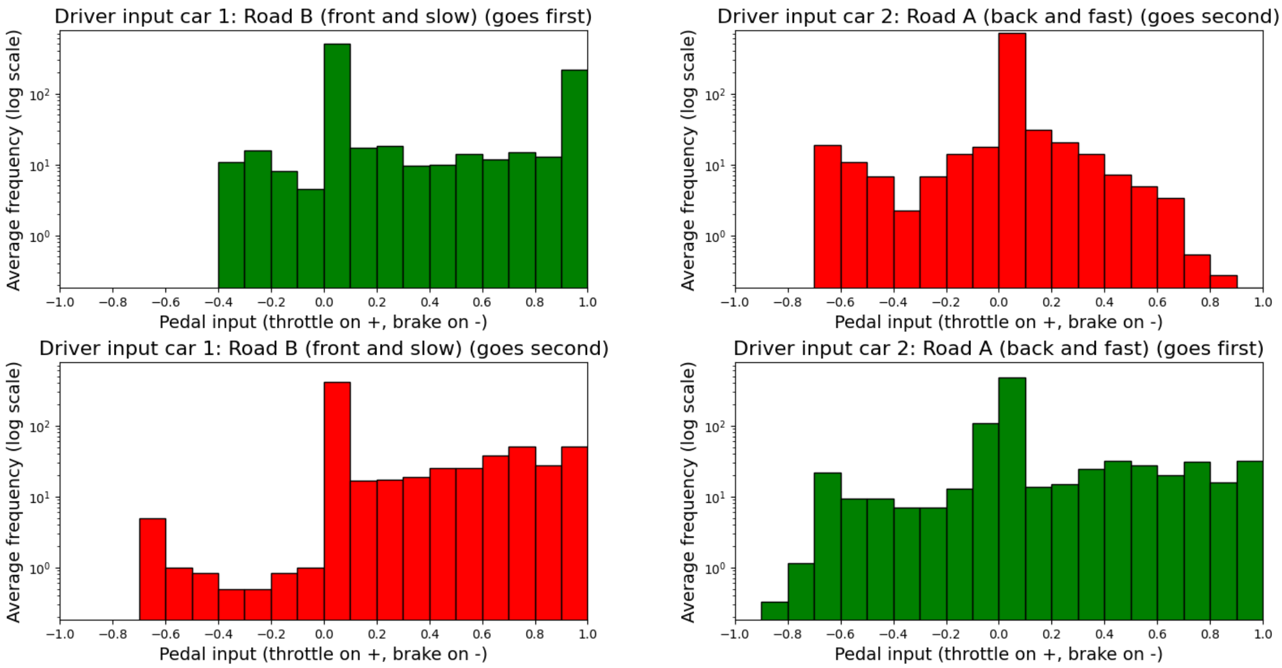

Figure 28: Average control input distribution for the condition where Car 1 on Road $\mathcal{B}$ starts *front and slow*. The x-axis represents normalized pedal input, with positive values indicating throttle and negative values indicating braking. The y-axis shows average frequency on a logarithmic scale. The top left plot shows input for Car 1 when it goes first (green), and the bottom left shows the same condition when Car 1 goes second (red). The right side reflects the opposite condition—Car 2 on Road $\mathcal{A}$ starts *back and fast*. The top right shows Car 2 when yielding (red), and the bottom right when going first (green).

Appendix C: Trajectories

Appendix C illustrates the vehicle trajectories from two trials under the same condition. The first figure (Figure 30) in this appendix illustrates a case where Car 1 proceeds first, while the second figure (Figure 29) shows a trial in which Car 2 goes first. The differences in the sampled positions clearly demonstrate how drivers altered their trajectories based on what they observed from the other vehicle.

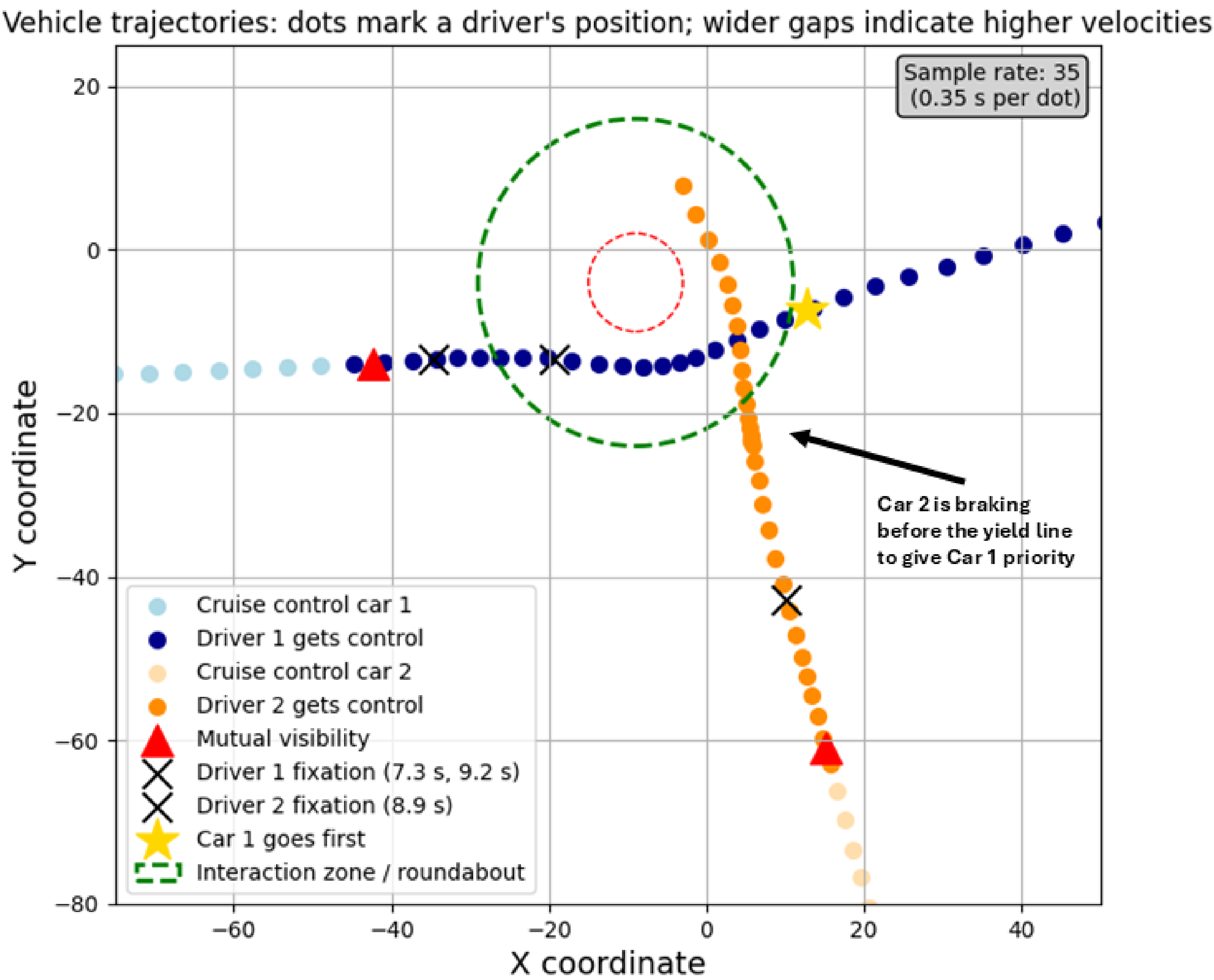

Figure 29: This figure is a larger version of Figure 14 for clarity. Vehicle trajectories for trial 121, with condition 3. Each dot represents a sampled vehicle position (0.35-second intervals). The blue and orange lines show the trajectories of Car 1 and Car 2, with light segments representing cruise control and dark segments representing manual control. Triangles indicate when mutual visibility occurred, black markers show the fixations and the green dashed circle denotes the interaction zone. The yellow star marks which car entered the conflict zone first. In this figure, Car 2 slows down before entering the conflict zone to allow Car 1 to pass first. This behavior follows the moment when the driver in Car 2 fixates on Car 1, indicating that the yielding decision was made after visual contact was established.

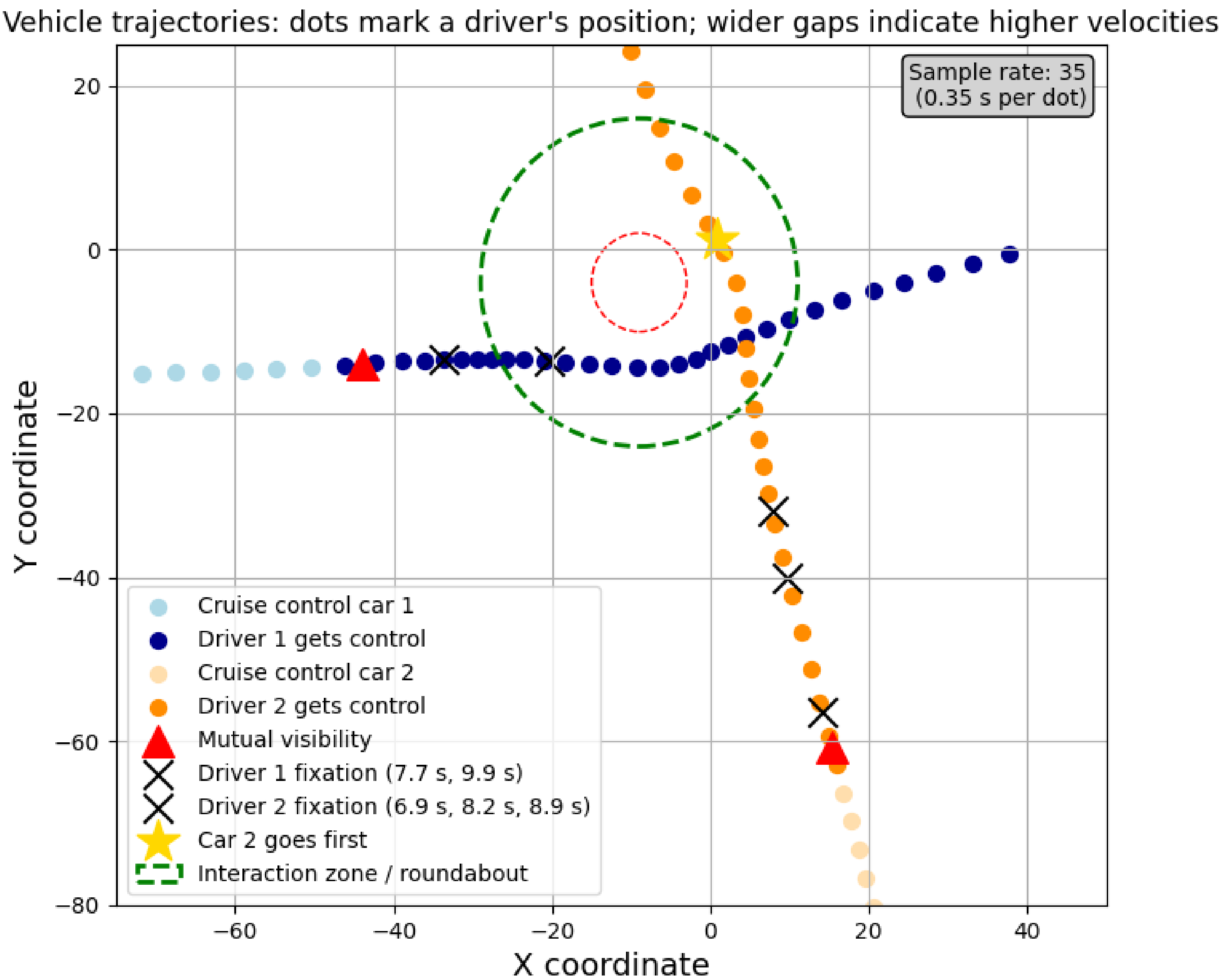

Figure 30: Alternative vehicle trajectory for trial 121, using the same condition as in Figure 14. In this trial, Car 2 proceeds first through the conflict zone. Each dot represents a sampled vehicle position (0.35-second intervals). Cruise control and manual control phases are shown in light and dark segments, respectively. Triangles mark when drivers gained mutual visibility, black markers indicate fixations and the green dashed circle outlines the interaction zone. The yellow star shows which car entered the conflict zone first. Here, Car 2 accelerates after fixating on Car 1, who yields by braking or slowing down. This suggests that the decision to proceed was made shortly after visual contact.

APPENDIX D: PROMPT USE OF LARGE LANGUAGE MODELS

During the writing process of this thesis, I used large language models (LLMs), such as ChatGPT, to improve language quality and to remove spelling and grammar mistakes. My usage followed the steps below:

1) **Wrote the content**
   I wrote each paragraph without focusing on grammar, spelling or sentence structure.
2) **Requested corrections**
   I inserted the text into ChatGPT and asked it to fix grammar mistakes, correct spelling and connect sentences more clearly.
3) **Adjusted sentence style**
   I asked the model to remove words ending in *–ing*, since those often reduced readability and flow. Specifically I asked to model to remove the use of the present participle.
4) **Checked the output**
   I read the revised paragraph sentence by sentence to confirm that the meaning matched my original intent and adjusted accordingly if needed.
5) **Applied the method throughout**
   I used this method for most of the paragraphs in the thesis to maintain consistent quality.

All AI-assisted changes were reviewed manually before adding them to the final version.